

Contents

| | | |
|----------|--|----------|
| 1 | Introducing Two-Dimensional Bose Gas | 1 |
| 1.1 | Low-dimensional Bose gases | 1 |
| 1.1.1 | General overview | 1 |
| 1.1.2 | Bose-Einstein condensate in the flat geometry | 4 |
| 1.1.3 | Homogeneous non-interacting Bose gas | 6 |
| 1.1.4 | Kosterlitz-Thouless transition | 7 |
| 1.1.5 | Non-interacting trapped Bose gas | 9 |
| 1.2 | Weakly interacting Bose gas | 10 |
| 1.2.1 | Weakly interacting regime | 10 |
| 1.2.2 | Elementary excitations and quasiparticles | 11 |
| 1.2.3 | Macroscopic framework of weakly interacting trapped Bose gas | 12 |
| 1.3 | Brief introduction of the T-Matrix | 15 |
| 1.3.1 | Quantum control of the interacting Bose gas | 16 |
| 1.3.2 | The attractive interaction limit | 19 |
| 1.4 | Dynamics of vortices in a 2D Bose fluid | 20 |
| 1.4.1 | Vortices as charged bosons | 23 |
| 1.4.2 | Quantum Monte Carlo Techniques (VMC and DMC) | 24 |
| 1.5 | Brief outline of the thesis | 26 |

| | | |
|----------|--|-----------|
| 2 | Scattering properties for 2D Bose gas | 29 |
| 2.1 | Coupling parameters in a mixture of condensed and thermal-bosons | 29 |
| 2.1.1 | The two-body T-matrix | 30 |
| 2.1.2 | The many-body T-matrix | 31 |
| 2.1.3 | Calculation of coupling parameters | 32 |
| 2.1.4 | Equilibrium properties in the two-fluid model | 34 |
| 2.1.5 | Coupling strength and its effect on equilibrium properties | 35 |
| 2.2 | Feshbach resonance in a 2D Bose gas | 39 |
| 2.2.1 | Overview on scattering theory | 39 |
| 2.2.2 | Feshbach resonances in the 2D coupling | 41 |
| 2.2.3 | Equilibrium properties as functions of the coupling | 42 |
| 2.2.4 | Repulsive coupling ($\eta > 0$) | 43 |
| 2.2.5 | Attractive coupling ($\eta < 0$) | 44 |
| 3 | Rotating 2D trapped Bose gas | 47 |
| 3.1 | Single vortex in a rotating 2D Bose gas | 47 |
| 3.1.1 | GP model that accomodates a single vortex | 48 |
| 3.1.2 | The energy of a vortex | 49 |
| 3.1.3 | Numerical result for single vortex | 50 |
| 3.2 | Density Functional Theory for many-vortex problem | 54 |
| 3.2.1 | Introduction | 54 |
| 3.2.2 | Density Functional Theory | 56 |
| 3.2.3 | Interacting auxiliary system : Bogoliubov approach | 59 |
| 3.2.4 | Application of DFT to N vortex problem | 62 |

| | |
|---|-----------|
| 4 Summary and Future Direction | 65 |
| 4.1 Summary and future directions | 65 |
| Bibliography | 77 |

Chapter 1

Introducing Two-Dimensional Bose Gas

1.1 Low-dimensional Bose gases

1.1.1 General overview

The exotic phenomena of Bose-Einstein condensation was first predicted by Einstein [1], generalizing the concept of earlier work of Bose [2] on the quantum statistics of photons to indistinguishable particles with integral spin. These particles, later known to be bosons obey the symmetrical property of wave function under the exchange of particles. In nature atoms are classified into bosons or fermions according to their spin properties or intrinsic angular momentum. Bosons have integral spin while fermions are half-integral spin particles and are described by anti-symmetric wave function. Pauli's exclusion principles prohibiting two fermions to occupy a same quantum state is also due to this anti-symmetric property. On the other hand the symmetric nature of bosons allow them to macroscopically occupy a given state.

The most illustrative example of bosonic behaviour of atoms is the process of Bose-Einstein Condensation (BEC) where at sufficiently low temperatures the bosons would become locked together in the lowest single-particle quantum state. Bosons that were distributed among many eigenstates plunge

macroscopically into the equilibrium ground state (lowest energy state) via a phase transition. At this stage the de Broglie waves of neighbouring atoms coalesce to form a giant matter-wave. For the three dimension (3D) geometry the condition for attaining BEC is to achieve a dimensionless phase space density of

$$\rho\lambda_{DB}^3 \geq 2.612 \quad (1.1)$$

where $\tilde{\rho}$ and λ_{DB} are the density of the system and de Broglie wave length respectively. One can also say that BEC occurs when the de Broglie wavelength becomes comparable with the interparticle distance $d = \rho^{-1/3}$.

BEC has been actively pursued over the last few decades in a variety of different systems. The initial drive in studying BEC focused on the interpretation of the collective (superfluid) behaviour of liquid ^4He . In this case however, the interactions between atoms are so strong that the depletion of the condensate is very large. To investigate the physics of BEC phase transition in detail experimentalists have sought to obtain the phenomena of BEC in a weakly-interacting systems, where the interactions do not mask the quantum statistical effects.

The first "true" Bose-Einstein condensate was created by Cornell, Wieman and co-workers at JILA on June 5, 1995 [3]. They did this by cooling a dilute vapor consisting of approximately 2000 rubidium-87 atoms to 170 nK, the lowest temperature ever achieved at that time, using a combination of laser cooling (a technique that won its inventors Steven Chu, Claude Cohen-Tannoudji, and William D. Phillips the 1997 Nobel Prize in Physics) and magnetic evaporative cooling. The Laser cooling was followed by cycles of evaporative cooling, a principle similar to the thermalization of a cup of coffee. Henceafter a peak appears at the centre of the density distribution of the atomic cloud, which can be imaged by a resonant absorption technique after a ballistic expansion of the cloud as it is released from the trap (See Fig. (1.1)).

About four months later, an independent effort led by Wolfgang Ketterle at

MIT created a condensate made of sodium-23 [4]. Ketterle's condensate had about a hundred times more atoms, allowing him to obtain several important results such as the observation of quantum mechanical interference between two different condensates. Cornell, Wieman and Ketterle won the 2001 Nobel Prize for their achievement. In that same year Bose condensate on lithium was also observed by the group at Rice led by Randy Hulet [5]

The initial results by the JILA, MIT and Rice groups have led to an explosion of experimental activity. For instance, the first molecular Bose-Einstein condensates were created in 2003 by teams surrounding Rudolf Grimm [6] at the University of Innsbruck and the first fermionic condensate by Deborah Jin and co-workers [7] at the University of Colorado at Boulder.

These pioneering realisation of BEC in a weakly-interacting system of trapped dilute alkali atoms in the mid 90's has revived the interest in the theoretical studies of Bose gases. A rather massive amount of work has been done in the last couple of years, both to interpret the initial observations and to predict new phenomena. In the presence of harmonic confinement, the many-body theory of interacting Bose gases gives rise to several unexpected features. This opens new theoretical perspectives in this interdisciplinary field, where useful concepts coming from different areas of physics (atomic physics, quantum optics, statistical mechanics and condensed-matter physics) are merging together.

Due to the enormous breadth of the subject, it is quite impossible to give a full coverage of the basic theory of Bose-Einstein condensation and its experimental realizations together with its many novel applications. A large series of reviews and books has already emerged elaborating in clear details this novel state of matter. Readers are recommended to retrieve informations from Pethick and Smith [8], Legget [9], Parkin and Walls [10], Griffin, Snoke and Stringari [11] and so on. This thesis is written for a specialist audience for those whom already acquainted with the basic theory of Bose-Einstein condensation in a 3D geometry. In spite of this, or rather because of this I

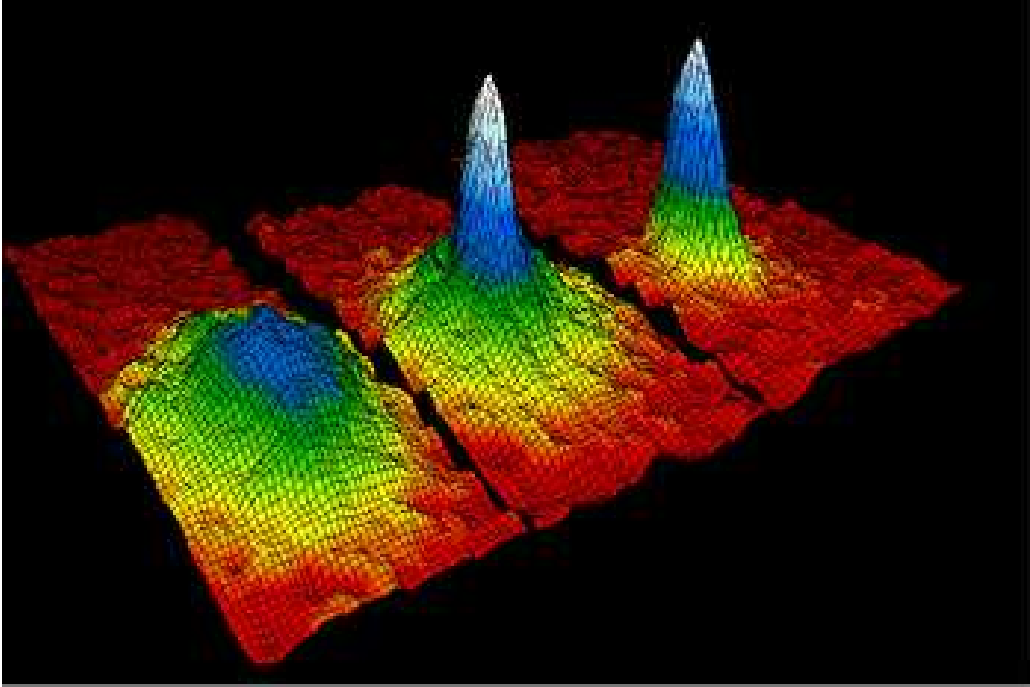


Figure 1.1: The first BEC in a gas of ^{87}Rb atoms, as it appears in two-dimensional time-of-flight images as temperature is decreased below T_c . Adapted from Anderson et. al. [3]

move ahead bypassing into the two-dimensional (2D) territories introducing the peculiarity phenomena arising in the squeezed flat geometry.

1.1.2 Bose-Einstein condensate in the flat geometry

The possibility of Bose-Einstein Condensation (BEC) phase transition occurring in a 2D geometry has a remarkable history and breakthroughs. The effect of dimensionality on the existence and character of BEC or superfluid phase transition has seen a spurt of interest in recent years. A peculiar feature of the low-dimensionality (1D or 2D geometry) at finite temperature is the absence of a 'true condensate' following the Bogoliubov k^{-2} theory, believed to be originated from the long wave-length phase fluctuations [12]. This has been proved in the seminal work of Mermin and Wagner [13] and Hohenberg [14].

Generally for a weakly interacting Bose gas at rest, the phenomenon of BEC is related to the macroscopic population of the single-particle state at zero momentum. One should expect a peak in the momentum distribution if condensation occur. One can also rely on the criterion first suggested by Onsager and Penrose [15] in the context of quantum field theory. They associated BEC with the emergence of long-range “off-diagonal” order in the one-body density matrix $\rho(\mathbf{r} - \mathbf{r}') = \langle \psi^\dagger(\mathbf{r})\psi(\mathbf{r}') \rangle$. Here $\psi(\mathbf{r})$ and $\psi^\dagger(\mathbf{r})$ are the annihilation and creation field operators for a particle at position \mathbf{r} and $\langle \dots \rangle$ is the mean value. It was shown by Hohenberg [14] that for two-dimensional Bose gas the correlation function depends algebraically on $|\mathbf{r} - \mathbf{r}'|$ with an exponent $\gamma(T)$ that varies proportionally with the temperature T as

$$\langle \psi^\dagger(\mathbf{r})\psi(\mathbf{r}') \rangle \sim |\mathbf{r} - \mathbf{r}'|^{\gamma(T)}. \quad (1.2)$$

Algebraic decay of the correlation function is what one expect when the temperature is tuned to the critical temperature of a continuous phase transition. In fact, this is known as the Kosterlitz-Thouless transition where the system cools toward a superfluid state through the binding of vortices with opposite vorticity [16]. Nevertheless in the limit $T \rightarrow 0$ global coherence is achieved in a homogeneous 2D system and a true condensate then exists. In contrast, for a trapped 2D fluid the modification of the density of states caused by the confining potential allows a true condensate to exists even at finite temperature.

Recent experiments have realized a quasi-two-dimensional (Q2D) cold Bose gas by tuning the anisotropy of the trapping potential [17, 18, 19, 20]. This achievement has attracted vast attention on the new physics appearing in the currently studied low- dimensional trapped gases and the nature of finite-size and finite-temperature effects.

1.1.3 Homogeneous non-interacting Bose gas

For a homogeneous gas, the individual particle eigenstates are characterized by momentum \mathbf{k} and corresponding eigenenergy $\epsilon_{\mathbf{k}} = \hbar^2 \mathbf{k}^2 / 2m$, where m is the mass of the particle. At thermal equilibrium with temperature T , a uniform gas of N bosons obeys the well-known Bose-Einstein distribution

$$f(\epsilon_{\mathbf{k}}, T) = \frac{1}{\exp((\epsilon_{\mathbf{k}} - \mu)/k_B T) - 1}, \quad (1.3)$$

where k_B is the Boltzmann constant and μ corresponds to the chemical potential of the system. The chemical potential can be interpreted as the energy required by a N -particle system to exchange one particle with its environment. The total number of particles in the excited states is given by the sum

$$N_{ex} = \sum_{\mathbf{k}} f(\epsilon_{\mathbf{k}}, T), \quad (1.4)$$

which specifies the value of the chemical potential μ . However, in a macroscopic system the volume is so large that the energy levels can be treated as continuous. Thus, Eq. (1.4) can be written in the integral form

$$N_{ex} = \tau \int d\epsilon_{\mathbf{k}} D(\epsilon_{\mathbf{k}}) f(\epsilon_{\mathbf{k}}, T) \quad (1.5)$$

with τ being the two-dimensional area and $D(\epsilon_{\mathbf{k}})$ is the density of state. In two-dimension, the smoothed density of state is $D(\epsilon_{\mathbf{k}}) = L^2 m / 2\pi \hbar^2$, where L^2 is the surface area. If we take the lower limit to be zero, then the integral does not exist because of the divergence at low energies. In a two-dimensional box, the ground state has energy $\epsilon_0 \sim \hbar^2 / mL^2$, since its wavelength is comparable to the linear extent of the area. To estimate the number of excited particles, we implement a cut-off (ϵ_0) in the integral as a lower bound. This gives us

$$N_{ex} \sim \frac{k_B T}{\epsilon_0} \ln\left(\frac{k_B T}{\epsilon_0}\right). \quad (1.6)$$

The number of excited particles becomes equal to the total number of particles at a temperature (critical temperature) given by

$$k_B T_c \sim \frac{\hbar^2}{mL^2} \frac{N}{\ln N} = \hbar^2 \frac{\tilde{\sigma}}{m \ln N}, \quad (1.7)$$

where $\tilde{\sigma} = N/L^2$ is the number of particles per unit area. For a large system and in the thermodynamic limit ($N \rightarrow \infty$), the transition temperature tends to zero. This indicates that the macroscopic occupation of particles can only occur at zero temperature for a uniformly large system in the thermodynamic limit. Hohenberg [14] has proposed an *ad absurdum* reasoning for the absence of off-diagonal long range order for in a 2D uniform Bose gas at finite temperature. In the presence of condensate the following inequality

$$n(\mathbf{k}) \geq -\frac{1}{2} + \frac{mk_B T}{\hbar^2 k^2} \frac{n_0}{n} \quad (1.8)$$

should hold, where $n(\mathbf{k})$ is the momentum distribution at low momenta, n_0 is the condensate density while n is the total density. However for 2D, the density of excited particles evaluated using the integral $n_{exc} = \int d^2\mathbf{k} n(\mathbf{k})$ diverges. So, one is led to the conclusion that the condensate fraction must be zero at any finite temperature.

1.1.4 Kosterlitz-Thouless transition

The theorem of Mermin and Wagner [13], which forbids the spontaneous breaking of a continuous symmetry in two-dimension due to the enhanced importance of long-wavelength thermal fluctuations, also reinforces the argument put forward by Hohenberg [14]. However, that a different kind of phase transition to a state with algebraic long-range order occurs in a 2D Bose fluid was first pointed out by Kosterlitz and Thouless [16]. This so called topological phase transition is associated with dissociation of a large number of vortex pairs and the immediate destruction of superfluidity caused by the phase slip process that occur once unbound vortices are present [21]. Nelson and Kosterlitz [22] predicted by means of a Renormalization-Group analysis that the discontinuous drop in the superfluid density n_s at the critical temperature T_c is of universal nature and such that $n_s \Lambda_c^2 = 4$, where Λ_c is the thermal de Broglie wavelength.

The Kosterlitz-Thouless transition can easily be demonstrated using the

two-dimensional XY-model. The model consists of planar rotors of unit length arranged on a two-dimensional square lattice. The Hamiltonian of the system is given by

$$H = -J \sum_{\langle i,j \rangle} \mathbf{S}_i \cdot \mathbf{S}_j = -J \sum_{\langle i,j \rangle} \cos(\phi_i - \phi_j) \quad (1.9)$$

where $J > 0$ and the sum $\langle i, j \rangle$ is over the lattice sites of nearest neighbours only. Here we take $|\mathbf{S}_i| = 1$ and ϕ_i is the angle that the i th spin makes with some arbitrary neighbours. Expanding about a local minima of H gives

$$H - E_0 \sim \frac{J}{2} \int d\mathbf{r} (\nabla \phi(\mathbf{r}))^2 \quad (1.10)$$

where $\phi(\mathbf{r})$ is a phase function defined over the lattice sites and E_0 is the non-vortex ground state. By spherical symmetric consideration and taking into account a quantized vortex configuration, we can estimate the energy of a single vortex E_{vor} to be

$$E_{vor} - E_0 \sim \pi J \ln(L/a_s) \quad (1.11)$$

where L is the finite system size and a_s is the lattice spacing. However, the free energy of a single vortex can be calculated using the Helmholtz free energy relation $F = E_{vor} - TS$, where S is the entropy estimated from the number of places where we can position the vortex center (in a classical viewpoint), namely on each of L^2 plaquette in a square lattice, *i.e.* $S = k_B \ln(L^2/a^2)$. Accordingly the free energy is given by

$$F = E_0 + (\pi J - 2k_B T) \ln(L/a_s). \quad (1.12)$$

For $T < \pi J/2k_B$ the free energy will diverge to plus infinity as $L \rightarrow \infty$. At temperatures $T > \pi J/2k_B$ the system can lower its free energy by producing vortices ($F \rightarrow -\infty$). This simple heuristic argument points to the fact that the logarithmic dependence on system size of the energy of the vortex combines with the logarithmic dependence of the entropy to produce the subtleties of the vortex unbinding transition. It is the logarithmic size

dependence of the two-dimensional vortex energy that allows the outcome of the competition between the entropy and the energy to change qualitatively at a certain finite critical temperature T_{KT} known as the Kosterlitz-Thouless transition.

In reality it is not the single vortices of the same signs that proliferate at a certain temperature. What happens is that the larger vortex pairs which are bound together for temperature below T_{KT} unbind at T_{KT} . This is a collective effect.

1.1.5 Non-interacting trapped Bose gas

Let us consider a symmetric harmonic confining potential $V(\mathbf{r}) = m\omega^2(x^2 + y^2)/2$ to describe the BEC cross-over of the 2D Bose gas. In this case the particle energy is $E_v = \hbar\omega(n_x + n_y)$, with quantum numbers n_x and n_y which are non-negative integers. The density of states for this system is then $D(E) = E/(\hbar\omega)^2$, and the contribution of low-energy excited states to the total number of particles is negligible. The ground state ($E = 0$) population is given by

$$N_0 = \frac{1}{\exp(-\mu/k_B T) - 1} \quad (1.13)$$

which becomes macroscopic even for a small negative μ . A cross-over to BEC regime exists in this case. Therefore, separating out the population of the ground state, one can replace the summation in Eq. (1.4) by an integration, and one gets

$$N = N_0 + V \int d\epsilon_{\mathbf{k}} D(\epsilon_{\mathbf{k}}) f(\epsilon_{\mathbf{k}}, T). \quad (1.14)$$

Using the relation $-\mu/k_B T \approx 1/N_0$, which is obtained using Eq. (1.13) assuming that ground state is macroscopically populated one can easily show that Eq. (1.14) gives the following result [23]:

$$N \left[1 - \left(\frac{T}{T_c} \right)^2 \right] = N_0 - \left(\frac{T}{\hbar\omega} \right)^2 \frac{1 + \ln N_0}{N_0}, \quad (1.15)$$

where $T_c = \sqrt{\frac{6N}{\pi^2}} \hbar\omega$ is the 2D BEC transition temperature for the non-interacting case. The effects of the interactions on this critical temperature

will be discussed in chapter 2.

1.2 Weakly interacting Bose gas

Preliminary works of Bogoliubov [24], Huang et al. [25, 26] and Lee et al. [27, 28] were mainly focused on the theory of interacting homogeneous Bose gases. The extension to inhomogeneous gases was first explored by Gross [29], Pitaevskii [30] and Fetter [31, 32]. The thermodynamic behaviour of trapped Bose gases has been already the object of several theoretical works, starting from the development of the Hartree-Fock formalism [33], the inclusion of interaction effects using the local density approximation [34, 35] up to the most recent approaches based on self-consistent mean-field theory [11, 36] and numerical simulation.

1.2.1 Weakly interacting regime

I will consider weakly interacting gases with a short-range potential of interaction between particles. The total interaction energy is equal to the sum of pair interactions in the c-number formalism and can be written as $E_{int} = N^2g/2A$, where g is the coupling constant for the pair interparticle interaction, N is the number of particles, and A is the area. Consequently, the interaction energy per particle is equal to $E_{int} = ng$, with n being the $2D$ density. The general criteria for a weakly interacting regime assumes that the mean interparticle separation \bar{r} greatly exceeds the characteristic radius of interaction between particles, l_e . In the $2D$ case we have $\bar{r} \sim (2\pi n)^{-1/2}$ and thus one obtain the inequality $n l_e^2 \ll 1$.

Another important condition for weakly interacting regimes is that the wavefunction is not influenced by the interaction between the particles if the interparticle distance is of order \bar{r} . Based on this condition, we can develop a physical picture which will be used for finding how the criterion of the weakly interacting regime depends on the dimensionality of the system.

For example let consider a box of size \bar{r} , which accomodates one particle in average. In the limit $T \rightarrow 0$, the particle kinetic energy is $E_{kin} \sim \hbar^2/m\bar{r}^2$. The wavefunction is not influenced by the interparticle interaction if the kinetic energy per particle is much larger than the interaction energy per particle. The inequality $E_{kin} \gg E_{int}/N$ immediately gives the criterion of weakly interacting regime in term of of the density and coupling constant. In the 2D case this criterion takes the form

$$\frac{m|g|}{2\pi\hbar^2} \ll 1. \quad (1.16)$$

where g is the 2D coupling constant which will be explained in detail in the next chapter. Most of the work in this thesis deals within the small repulsive/attractive limit ($g > 0$ or $g < 0$), except for the case where a weakly bound state of colliding atoms is present near resonance. Then the strength of g is extremely large and even at very low densities the criterion of Eq. (1.16) does not hold. Thus, one has to look for solutions beyond mean-field.

1.2.2 Elementary excitations and quasiparticles

The presence of a condensate mean field is naturally expected to affect the spectrum of the elementary excitations of a bosonic gas. This is a direct consequence of the fact that the atoms are not interacting with other individual atoms, but they are moving dominantly in the presence of a coherent condensate field. As expected, the deviation from the non-interacting spectrum become more pronounced as more particles are added to the condensate, since this lead to an increase in density. The notion of an excited (bare) atom interacting with condensed atoms leads quite generally to the idea of a dressed atom, or quasi-particle. One can see the significance of interactions to the change in the spectrum of elementary excitations by looking at the quasi-particle dispersion relation given by [24]

$$\hbar\omega_k = \sqrt{\epsilon_k^2 + 2n_c V_0 \epsilon_k} \quad (1.17)$$

where $\epsilon_k = \hbar^2 k^2 / 2m$ corresponds to the non-interacting energy spectrum, n_c is the condensate density and V_0 is the Fourier transform of the interaction potential in the limit $\mathbf{k} \rightarrow 0$.

Recently, it was demonstrated by Al Khawaja et. al [37] that by taking the following modified type excitation spectrum:

$$\hbar\omega_k = \sqrt{\epsilon_k^2 + 2\mu\epsilon_k} \quad (1.18)$$

where $\mu = n_c T^{2B}(-2\mu)$, one is able to avoid the dangerous ultraviolet and infrared divergences in the 2D Bose gas. $T^{2B}(-2\mu)$ is the multi-loop two-body T-matrix taken at energy argument -2μ which is exactly what it costs to excite two atoms out of the condensate (See Sec. 1.3 for more details).

1.2.3 Macroscopic framework of weakly interacting trapped Bose gas

Let us consider the Bose gas trapped in a 2D isotropic planar trap $V(\mathbf{r}) = m\omega_{\perp}^2(x^2 + y^2)/2$. The starting point is the grand-canonical Hamiltonian in second quantization language:

$$H = H_0 + \frac{1}{2} \int d\mathbf{r} \int d\mathbf{r}' \psi^{\dagger}(\mathbf{r})\psi^{\dagger}(\mathbf{r}')V(\mathbf{r} - \mathbf{r}')\psi(\mathbf{r}')\psi(\mathbf{r}) \quad (1.19)$$

where $H_0 = \int d\mathbf{r}\psi^{\dagger}(\mathbf{r}) \left[-\frac{\hbar^2}{2m}\nabla^2 + V(\mathbf{r}) - \mu \right] \psi(\mathbf{r})$, μ is the chemical potential and $V(\mathbf{r} - \mathbf{r}')$ is the interatomic interaction potential. The annihilation and creation operators are denoted by $\psi^{\dagger}(\mathbf{r})$ and $\psi(\mathbf{r}')$ respectively and obey the Bose- Einstein commutation relation

$$[\psi(\mathbf{r}), \psi^{\dagger}(\mathbf{r}')] = \delta(\mathbf{r} - \mathbf{r}') \quad [\psi(\mathbf{r}), \psi(\mathbf{r}')] = [\psi^{\dagger}(\mathbf{r}), \psi^{\dagger}(\mathbf{r}')] = 0. \quad (1.20)$$

Since we are looking at system at very low temperature, only the contribution of s-wave scattering is important. Consequently we neglect the momentum dependence of the interatomic interaction and use $V(\mathbf{r} - \mathbf{r}') = V_0\delta(\mathbf{r} - \mathbf{r}')$. This leads to ultraviolet divergences but can be easily remedied. I will illustrate the technique in the next chapter. However with this contact potential

the above Hamiltonian will reduce to the following one,

$$H = H_0 + \frac{1}{2} \int d\mathbf{r} V_0 \psi^\dagger(\mathbf{r}) \psi^\dagger(\mathbf{r}) \psi(\mathbf{r}) \psi(\mathbf{r}). \quad (1.21)$$

The time-dependent Heisenberg operator $\psi(\mathbf{r}, t) = \exp(iHt/\hbar)\psi(\mathbf{r}) \exp(-iHt/\hbar)$ obeys the equation of motion

$$i\hbar \frac{\partial \psi(\mathbf{r}, t)}{\partial t} = [\psi(\mathbf{r}, t), H] \quad (1.22)$$

which yields the non-linear operator equation

$$i\hbar \frac{\partial \psi(\mathbf{r}, t)}{\partial t} = \left(-\frac{\hbar^2}{2m} \nabla^2 + V(\mathbf{r}) \right) \psi(\mathbf{r}, t) + g \psi^\dagger(\mathbf{r}, t) \psi(\mathbf{r}, t) \psi(\mathbf{r}, t). \quad (1.23)$$

By separating out the condensate part of the particle field operator one can write $\psi(\mathbf{r})$ as a sum of spatially varying condensate wavefunction $\Psi(\mathbf{r})$ and a fluctuation field operator $\tilde{\psi}$,

$$\psi = \Psi(\mathbf{r}) + \tilde{\psi}. \quad (1.24)$$

The wave function $\Psi(\mathbf{r})$ is also known as the order parameter and is defined as the statistical average of particle field operator $\Psi(\mathbf{r}) = \langle \psi \rangle$.

Using the decomposition in Eq.(1.24) above, one can write the interaction term $\psi^\dagger(\mathbf{r}, t)\psi(\mathbf{r}, t)\psi(\mathbf{r}, t)$ of Eq.(1.23) in the form

$$\psi^\dagger(\mathbf{r}, t)\psi(\mathbf{r}, t)\psi(\mathbf{r}', t) = |\Psi|^2\Psi + 2|\Psi|^2\tilde{\psi} + \Psi^2\tilde{\psi}^\dagger + \Psi^*\tilde{\psi}\tilde{\psi} + 2\Psi\tilde{\psi}^\dagger\tilde{\psi} + \tilde{\psi}^\dagger\tilde{\psi}\tilde{\psi}. \quad (1.25)$$

Taking the average of the above relation one obtains

$$\langle \psi^\dagger(\mathbf{r}, t)\psi(\mathbf{r}, t)\psi(\mathbf{r}, t) \rangle = n_c\Psi + \tilde{m}\Psi^* + 2n_{nc} + \langle \tilde{\psi}^\dagger\tilde{\psi}\tilde{\psi} \rangle, \quad (1.26)$$

where $n_c = |\Psi|^2$ is the condensate density, $n_{nc} = \langle \tilde{\psi}^\dagger\tilde{\psi} \rangle$ is the non-condensate density while $\tilde{m} = \langle \tilde{\psi}\tilde{\psi} \rangle$ is the off-diagonal (anomalous) density. So taking the average for Eq. (1.23) and using the relation in Eq. (1.26) we arrive at the equation of motion for $\Psi(\mathbf{r}, t)$:

$$\begin{aligned} i\hbar \frac{\partial \Psi(\mathbf{r}, t)}{\partial t} &= \left(-\frac{\hbar^2}{2m} \nabla^2 + V(\mathbf{r}) + gn_c(\mathbf{r}, t) + 2gn_{nc}(\mathbf{r}, t) \right) \Psi(\mathbf{r}, t) \\ &+ g\tilde{m}\Psi^* + g \langle \tilde{\psi}^\dagger\tilde{\psi}\tilde{\psi} \rangle \end{aligned} \quad (1.27)$$

Neglecting the three-field correlation function $\langle \tilde{\psi}^\dagger \tilde{\psi} \tilde{\psi} \rangle$ in the equation above is called the Hartree-Fock-Bogoliubov (HFB) approximation. Further simplification to that by ignoring the term $\tilde{m} = \langle \tilde{\psi} \tilde{\psi} \rangle$ is known as Hartree-Bogoliubov-Popov (HBF-P) approximation. In this thesis I will refer to the static Popov limit in which the fluctuation of the thermal cloud is ignored $n_{nc}(\mathbf{r}, t) \sim n_{nc}(\mathbf{r})$ and will only consider a stationary solution for $\Psi(\mathbf{r}, t) = \Psi(\mathbf{r}) \exp(-i\mu t/\hbar)$. Thus the Non-linear Schrödinger equation Eq. (1.27) leads to the Gross-Pitaevskii (GP) equation

$$\left(-\frac{\hbar^2}{2m} \nabla^2 + V(\mathbf{r}) + g_2 n_c(\mathbf{r}) + 2g_1 n_{nc}(\mathbf{r}) \right) \Psi(\mathbf{r}) = \mu \Psi(\mathbf{r}). \quad (1.28)$$

As anticipated, the general finite temperature GP equation above is not closed. Its solution requires one to know the information about the distribution of the non-condensate particles. Readers should also be aware that in the above equation I have introduced g_1 and g_2 which represent the coupling parameters due to condensate-noncondensate and condensate-condensate repulsion respectively. This choice of coupling parameters in studying the equilibrium property of condensate-thermal particles is the core issue of this thesis. Coming back to the problem of thermal density distribution, I will take a semi-classical approximation [38] supplemented with a Hartree-Fock type energy spectrum

$$\epsilon(\mathbf{p}, \mathbf{r}) = \frac{p^2}{2m} + V_{ext}(\mathbf{r}) + 2g_1 n_c(\mathbf{r}) + 2g_1 n_{nc}(\mathbf{r}). \quad (1.29)$$

Hence, the thermal density is obtained by integrating out the momentum

$$\begin{aligned} n_{nc}(\mathbf{r}) &= \int \frac{d\mathbf{p}}{(2\pi\hbar)^2} f(\epsilon(\mathbf{p}, \mathbf{r}), T) \\ &= -\frac{m k_B T}{2\pi\hbar^2} \times \ln [1 - \exp(\beta(\mu - V_{eff}(\mathbf{r})))] . \end{aligned} \quad (1.30)$$

where we consider the effective potential as $V_{eff}(\mathbf{r}) = V(\mathbf{r}) + 2g_1 n_c(\mathbf{r}) + 2g_1 n_{nc}(\mathbf{r})$. This type of method that couples solution of condensate and non-condensate density is also known as the Two-Fluid model.

1.3 Brief introduction of the T-Matrix

To describe the microscopic treatment of binary collisions, one generally considers the interaction between two condensed atom in a dilute weakly-interacting BEC. The complete set of two-particle interactions can be summed up into a single operator called the Transition matrix or simply T-matrix. This operator can be determined via a perturbation theory expansion in term of the actual interatomic potential. The possible scattering events can be described by a single interaction $\langle \mathbf{k}' | V | \mathbf{k} \rangle$, or alternatively the particles may first make a transition to an intermediate state $|\mathbf{q}\rangle$ before interacting again to emerge in the state $|\mathbf{k}'\rangle$. The repeated form of the scattering from initial to a final state via the intermediate state $|\mathbf{q}\rangle$ can be defined as an expansion of the T operators in term of the actual interatomic potential V via

$$T = V + VG^0V + VG^0VG^0V + \dots \quad (1.31)$$

where $G^0 = (z - H^0)^{-1}$ corresponds to the unperturbed Green's function and H^0 is the free Hamiltonian in the absence of interactions while z corresponds to the centre-of-mass-energy of for the pair of atoms. In practice, the T operator can be assembled more explicitly in term of the Lippman Schwinger relation (see also in Sec. 2.1.1).

$$T = V + VG^0T. \quad (1.32)$$

The two-body interaction above describe collision in *vacuo* in which the intermediate states are single-particle in nature. In order to illustrate the interaction within a two-dimensional BEC we must consider the scattering in the presence of condensate particles. Interactions of this nature can be described by the many-body T-matrix $T^{MB}(\mathbf{k}, \mathbf{k}', \mathbf{K}; z)$ which due to the surrounding particles depends also on the center-of-mass momentum \mathbf{K} of the colliding particles. In the zero momentum limit we set $\mathbf{k}', \mathbf{k}, \mathbf{K} = 0$. Since we are interested in the matrix element with all momenta equal to zero we find to a good approximation the following Bethe-Salpeter equation for

the scattering of a quasi-particle,

$$\begin{aligned}
 T^{MB}(\mathbf{k}, 0, 0; z) &= V(\mathbf{k}) + \frac{1}{\tau} \sum_{\mathbf{k}'} V(\mathbf{k}') \frac{1 + 2N(\hbar\omega_{\mathbf{k}'})}{z - 2\hbar\omega_{\mathbf{k}'}} \\
 &\times T^{MB}(\mathbf{k}', 0, 0; z)
 \end{aligned}
 \tag{1.33}$$

where $\hbar\omega_{\mathbf{k}}$ is the quasi-particle energy defined in Eq. (1.18) and $N(x) = 1/(\exp(\beta x) - 1)$ is the Bose-Einstein distribution function. However in the zero momentum limit, the above Bethe-Salpeter equation is tainted by an ultraviolet divergence due to the neglect of the momentum dependence of the potential $V(\mathbf{k})$. This divergence is remedied by using the following relation,

$$\frac{1}{T^{2B}(0, 0; \bar{z})} = \frac{1}{V(0)} + \frac{1}{\tau} \sum_{\mathbf{k}} \frac{1}{2\epsilon_{\mathbf{k}} - \bar{z}}
 \tag{1.34}$$

where $\bar{z} = -j\mu$ with $j = 1, 2$ depending whether the collision is between two condensate atoms ($j = 2$) or between one condensate and one non-condensate atom ($j = 1$). The details are given in Sec. 2.1. The collision between condensate and the thermal atoms become more probable as temperature increases. It is a crucial point and covers our investigation on the effect of interaction in calculating the density profiles at finite temperature (See Chapter 2).

1.3.1 Quantum control of the interacting Bose gas

A Feshbach resonance occurs when the energy of a metastable molecular state E_{res} matches the energy of a pair of incoming condensate atoms E_{th} and a coupling exists between them during a collisional process [39]. As described in the previous section, the scattering of particles with zero relative energy or momentum is specified by the scattering amplitude related to the T matrix. If the energy of the incoming particles E_{th} is close to the resonance energy E_{res} of one particular bound state (resonance state $|\psi_{res}\rangle$), the contributions from all other states will vary slowly with energy and they may be represented by non-resonant scattering length a_{bg} whose energy dependence is much weaker

compared to the resonance term. By writing the T matrix elements as a function of scattering length and using the argument discussed above we obtain the following relation,

$$T^{MB}(0, 0, 0) = T_{bg}^{MB}(0, 0, 0) + \frac{C(B)}{E_{th} - E_{res}}. \quad (1.35)$$

where T_{bg}^{MB} is the off-resonant scattering amplitude and $C(B)$ is the resonant width, weakly dependent on B . The total scattering amplitude that includes resonant and non-resonant terms for a 3D Bose can be easily calculated as $T^{MB}(0, 0, 0) \sim T^{2B}(0, 0, 0) = 4\pi\hbar^2 a/m$ by the two-body scattering of particles within the Born approximation [8]. Eq. (1.35) displays the energy dependence of the two-body T matrix and is characteristic of a Feshbach resonance. Hence the atomic interactions may be tuned by exploiting the fact that energies of the states depend on external parameters among which are the strength of a magnetic field. Expanding the energy denominator about the value of magnetic field we find

$$E_{th} - E_{res} \approx (\mu_{res} - 2\mu_i)(B - B_0), \quad (1.36)$$

where $\mu_i = -\frac{\partial \epsilon_i}{\partial B}$, $i = 1, 2$ are the magnetic moments of the two atoms in the open channel while $\mu_{res} = -\frac{\partial E_{res}}{\partial B}$ is the magnetic moment of the molecular bound state. Substituting Eq. (1.36) into Eq. (1.35) one obtains [39]

$$a(B) = a_{bg} \left(1 - \frac{C(B)}{B - B_0} \right). \quad (1.37)$$

where a_{bg} is the off-resonant scattering length. By sweeping across the magnetic field around the resonance location B_0 the coupling strength of the condensate can be used as a controlling tool. Hence one has the possibility not only to control the scattering length from a strongly repulsive to a strongly attractive regimes but also in obtaining a novel molecular condensate [6] (as depicted in Fig (1.2)).

Whether we can have a similar control of the interaction parameters for the strictly 2D condensate when the s -wave scattering length becomes larger

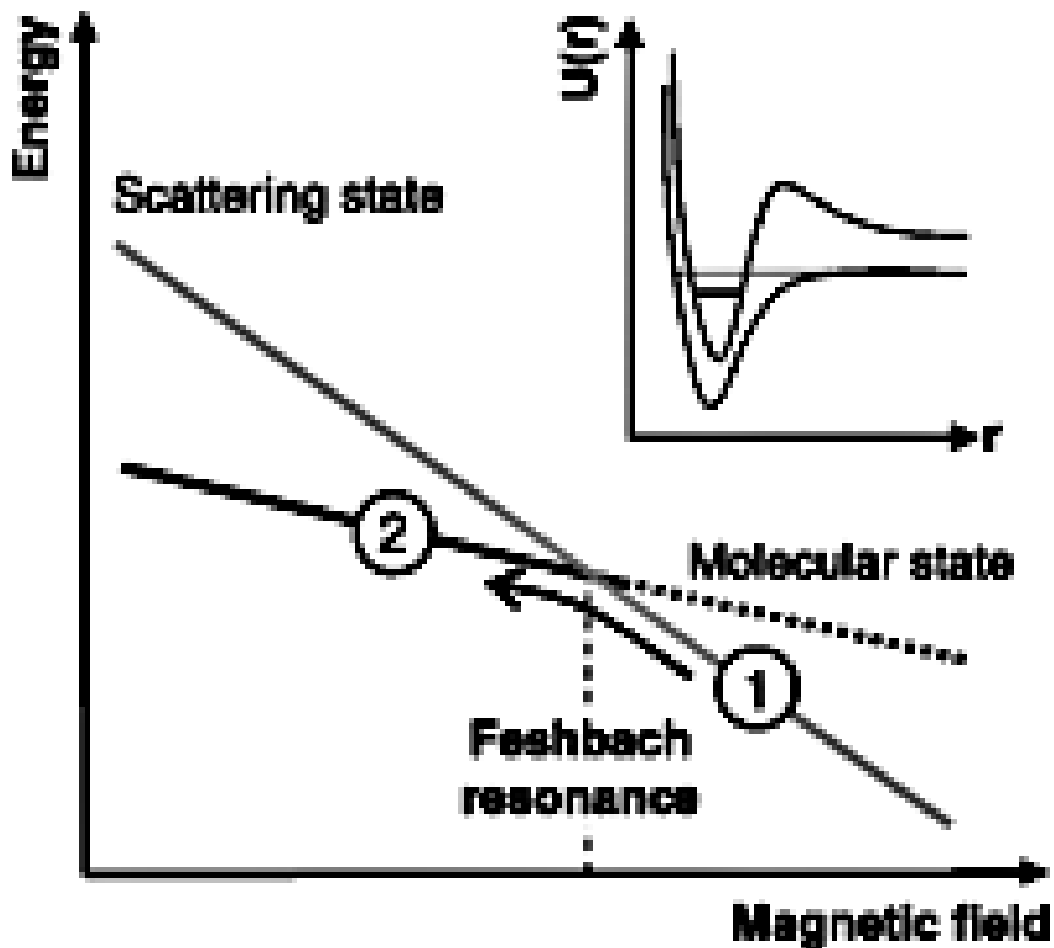


Figure 1.2: Energy diagram for the atomic scattering state and the molecular bound state. The Feshbach resonance condition occurs near 20 G, where the Zeeman energy of the atomic scattering state becomes equal to that of a molecular bound state because of the difference in magnetic moments. Molecules at (2) are created from the BEC at (1) by a downward sweep of the magnetic field across the resonance. For detection, a reversed sweep brings the molecules above the dissociation limit. The inset schematically shows the molecular potential that corresponds to the open channel (lower curve) and the molecular potential that supports the bound state (upper curve). U , potential energy; r , interatomic distance. From Herbig et. al. [6]

than the width of the axial trapping [40, 12] will be addressed in the second part of chapter 2. To my knowledge, I have not encountered any attempts to study the Feshbach resonances for a strictly 2D Bose gas. This motivated me to look into such phenomena in those low-dimensional regime by using the similar technique conventionally used in studying them in the 3D case.

Once a tunable coupling parameter is calculated it will be incorporated into the 2D dynamical GP equation to study the effect of the interactions on the density profiles at absolute zero temperature. I will perform a similar analysis as done by Kagan *et.al* [41] by modifying the coupling strength as a dimensionless physical parameter η which is defined as the ratio between the mean-field interaction energy and the harmonic-oscillator level spacing. The interaction is of repulsive nature if $\eta > 0$, else it is attractive for $\eta < 0$. The magnitude $\eta \ll 1$ indicates that we are in the weakly repulsive (attractive) regime and $\eta \gg 1$ means a strongly repulsive (attractive) for $\eta > 0$ ($\eta < 0$).

1.3.2 The attractive interaction limit

For an attractive interaction between particles ($\eta < 0$), the picture changes drastically. A Bose condensate with $|\eta| \gg 1$, in which the structure of the trap levels is not important, cannot be formed at all, since in this case the accumulation of particles in one quantum state would be associated with increase in energy [41]. In this case the dominant elastic pair collision will prevent the formation of a Bose condensate with densities $(n_c/n_o)\eta \gg 1$, since the structure of trap levels is essentially smeared out by interatomic interaction and there is no gap for the excitation of particles from the condensate.

As a simple illustration, by taking the TF approximation to Eq. (1.28) (assuming $n_{nc} = 0$ at $T = 0$) in this limit ($|\eta| \gg 1$) and substituting $\eta = -k^2$ where k is any positive number, we obtain the relation

$$\left| \frac{\Psi(\mathbf{r})}{\Psi(0)} \right| \sim \sqrt{1 + \frac{1}{2} \left(\frac{r}{k} \right)^2}. \quad (1.38)$$

What we have obtained is a monotonically increasing function which is not physical. The use of Eq.(1.28) is inappropriate to analyse the behaviour of a condensate with attractive interaction. Consequently, we need to incorporate the physics of atom losses due to three-body recombination and formation of metastability condensate in the attractive regime as investigated by several authors [41, 42, 43, 44] for the 3D case.

In order to model atom loss due to three-body recombination we add a phenomenological term proportional to the density squared $|\Psi(x)|^2$ with coefficient $K_3/2$ [45]. The GP equation which incorporates a three-body loss term reads

$$i\hbar\frac{\partial\Psi(r,t)}{\partial t} = \left[-\frac{\hbar^2}{2m}\nabla^2 + V_{ext} + gn_c - \frac{i\hbar K_3}{2}n_c^2 \right] \Psi(r,t), \quad (1.39)$$

where the rate coefficient K_3 is related to the atom loss rate given by :

$$\frac{dN}{dt} = -K_3 \int n_c^3 d\mathbf{r}. \quad (1.40)$$

A meta-stable solution of the above Eq. (1.39) exist only if one chooses a number N such that $N < N_c$ where N_c is the critical number as reported for the 3D case [46, 47, 48, 49]. Beyond this number, the system would begins to collapse and lead to infinite density fluctuation to form hydrodynamic 'Black hole' [49]. The calculation of this critical number for the 2D case is reported in chapter 2.

1.4 Dynamics of vortices in a 2D Bose fluid

Under appropriate stabilization conditions, such as steady applied rotation, vortices can form a regular array. In a rotating uniform superfluid, quantized vortex lines parallel to the axis of rotation form a Wigner-type crystal lattice [50]. At non-zero temperature, dissipative mutual friction from the normal component ensures that the array rotates with a same angular velocity as the container. A triangular vortex array is energetically favoured for vortices

near the rotation axis of rapidly rotating vessels of superfluid helium, (see Tkachenko [51, 52]).

However, the properties of vortices in a Bose-Einstein atomic condensate atoms have proven to be more tractable compared to the superfluid helium. Following the creation of single vortex lines in an atomic condensate by a phase imprinting technique [53], large arrays have been created via mechanical rotation and stirring of the condensate with laser beam [54, 55, 56]. The recent observation of Tkachenko modes (collective excitations) in the Bose-condensed ^{87}Rb condensate by Coddington et al. [57] stimulated more work on this direction. Congruent to that, there has been an enormous number of theoretical studies in analysing the properties of vortex lattices [58, 59, 60, 61], Tkachenko lattice oscillations (waves)[62, 63], the transition into a novel properties of Fractional Quantum Hall Effects (FQHE) and strongly correlated uncondensed liquid [64, 65].

Atomic Bose condensates allow one to study superfluids over a range of rotational frequencies Ω [55, 56, 66]. Baym [62] has classified four distinct physical regimes as Ω increases: (1) The 'stiff' Thomas-Fermi regime, where Ω is small compared with the lowest compressional frequencies, sk_0 , where s is the sound velocity, $k_0 \sim 1/R$ is the lowest wave number in the finite geometry, and R is the size of the system transverse to the rotation axis. The system is an incompressible fluid in this regime responding effectively to rotation. (ii) In the limit $sk_0 \ll \Omega \ll ms^2$, the system is said to be in a 'soft' Thomas-Fermi regime. Here the vortex core size is much smaller than inter-vortex spacing. (iii) When $\Omega \gg ms^2$, we enter a fast rotation regime where one is ensured that for a large vortex density, the intervortex separation is greater than the coherence length. This idea follows from the work of Baym [67] who showed shrinking of vortex cores when such limit is reached. In this rapidly rotating regime the system enters a effectively two-dimensional strong field. Viefers et al. [68] have shown that as the angular momentum of N particle system gets larger, particles are spread out in space and the 'Yrast line' (the lowest possible interaction energy for a given angular

momentum L) decreases. As the Yrast line decreases, the density of particle also decreases in parallel. Ho [58] on the other hand has predicted that in this limit particles should condense into the Lowest Landau Level (LLL) in the Coriolis force, similarly to charged particles in the quantum Hall regime. At relatively low vortex density, the vortices form a triangular lattice [51, 52] which is energetically favourable. There is a gap in the energy levels $\sim 2\omega_{\perp}$ when LLL is achieved. The single particle wave-function in the LLL has the form $\phi_i(r) \sim z^i \exp(-r^2/2d_{\perp}^2)$ where $z = x + iy$, $i=0,1,2,\dots$ and d_{\perp} is the transverse oscillator length given by $\sqrt{\hbar/m\omega_{\perp}}$. The LLL condensate wave-function is a linear superposition of such states :

$$\Phi_{LLL}(r) \sim \sum_i c_i z^i \exp(-r^2/2d_{\perp}^2) \sim \prod_{i=1}^N (z - z_i) \exp(-r^2/2d_{\perp}^2) \quad (1.41)$$

(iv) Eventually the vortex lattice melts [69, 65] and the system enters a strongly correlated vortex liquid [59, 68, 70, 64]. The melting is somehow controlled by a dimensionless Lindemann parameter

$$c_L = \frac{\Omega}{\pi\rho} = \left(\frac{d}{l_v}\right)^2 = \frac{n_v}{\rho} \quad (1.42)$$

where $d \equiv \rho^{-1/2}$ is the inter-particle distance, $l_v = \sqrt{\pi/\Omega}$ is the mean inter-vortex spacing and n_v ($n_v = \Omega/\pi$) is the density of vortices.

This parameter controls the relative strength of the quantum fluctuations and the melting transition into quantum Hall regime at zero temperature. The melting filling factor calculated using various methods [60, 65, 69] is found to be $c_L = (c_L)_m \sim 0.1$. The vortices are in the lattice phase if $c_L < (c_L)_m$, otherwise in molten phase if $c_L > (c_L)_m$. One could also say that the vortex crystal starts melting as the vortices begin to depart from their lattice positions.

However in this work, I am taking a completely diverse approach from the one discussed above. The difference is two-fold, firstly I am already in a 2D geometry so that an ultra-fast rotation to achieve this geometry is not required. Secondly I assume my vortices are in the liquid phase. Freezing

and strongly correlations need to be analyzed hence after. The following sections will shed more light on my approach to the N vortex problem in the confined 2D geometry.

1.4.1 Vortices as charged bosons

Let us consider a system of N bosons in a condensate confined within a cylindrical potential (with radial ω_{\perp} and axial trap frequencies Ω_z) and put into rotation with angular velocity Ω . The Hamiltonian of the system reads [9, 65]

$$\begin{aligned}
 H_{\Omega} &= \sum_{i=1}^N \frac{\mathbf{p}_i^2}{2m} + \frac{1}{2} m \omega^2 \mathbf{r}_i^2 - \Omega \hat{z} \cdot \mathbf{r}_i \times \mathbf{p}_i + \sum_{i<j=1}^N V(\mathbf{r}_i - \mathbf{r}_j) \\
 &= \sum_{i=1}^N \frac{(\mathbf{p}_i - m\Omega \hat{z} \times \mathbf{r}_i)^2}{2m} + \frac{1}{2} m [(\omega_{\perp}^2 - \Omega^2) r_{\perp}^2 + \Omega_z^2 z_i^2] \\
 &+ \sum_{i<j=1}^N V(\mathbf{r}_i - \mathbf{r}_j).
 \end{aligned}$$

This system is identical to a system of charge- Q particles interacting under the influence of a magnetic field

$$B^* = \nabla \times (m\Omega \hat{z} \times \mathbf{r}/Q) = (2m\Omega/Q) \hat{z}.$$

At sufficiently low temperatures and in the fast rotation limit $\Omega \gg ms^2$, this system enters an effectively two-dimensional strong field and the dissipation due to scattering of thermal excitations on the vortices is negligible, thus the vortex dynamics is conservative. The situation considered then corresponds to the Magnus-force dominated limit of vortex motion in a very clean superconductor [71, 72].

An indirect connection to the above argument can be related to the work of Nelson et al. [73] who have shown that the statistical mechanics of the flux-line lattice (FLL) of high- T_c superconductors can be studied through an appropriate mapping onto the 2D Yukawa boson system. Following this magnificent idea, Magro and Ceperley [74, 75] have performed Diffusion Monte

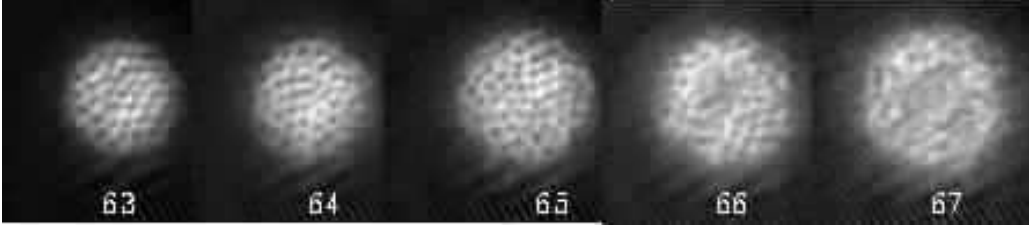


Figure 1.3: Vortices when rotation $\Omega \rightarrow \omega_{\perp}$. Centrifugal and trapping energy compensate and spatial extent becomes large. Adapted from Bretin et. al. [76]

Carlo (DMC) and Variational Monte Carlo (VMC) numerical calculations to calibrate the vortex properties for a homogeneous 2D Yukawa boson system. Taking a similar step, I will treat the system of N_v vortices as N bosons confined in a 2D harmonically planar trap $\frac{1}{2}m\omega_{\perp}^2 r^2$ performing a Density functional theory (DFT) calculation (See Chapter 3.)

1.4.2 Quantum Monte Carlo Techniques (VMC and DMC)

My DFT calculation heavily relies on the accurate data of VMC calculation of Magro and Ceperley [74]. So I feel it is necessary to display here some idea of what the method is all about. VMC method is a technique developed to minimize the ground-state energy of a many-body trial function. The energy functional $E = \langle \phi_T | H | \phi_T \rangle$, where ϕ_T is a family of trial functions is minimized by one of its particular choice of wave-function ϕ_0 known as the ground state. In other word we introduce a family of trial function $\phi(x, p)$, depending on the parameter p and compute the corresponding energy,

$$E(p) = \frac{\int \phi^*(p, r) H \phi(p, r)}{\int \phi^*(p, r) \phi(p, r)} \quad (1.43)$$

and look for the choice of $p = p^*$ such that E^* is the minimum energy within the parameter space. Obviously the success of VMC depends largely on a good choice of trial function. The most commonly used trial function when one is interested in identifying the solid or liquid phases of a system is the

Jastrow pair product which reads [74]

$$\phi_T = \prod_{i < j} \exp[-u(r_{ij})] \prod_i \exp[-c(\mathbf{r}_i - \mathbf{Z}_i)^2] \quad (1.44)$$

where \mathbf{r}_i is the position of *i*th of N particles, \mathbf{Z}_i are the lattice sites, r_{ij} is an interparticle distance, and $u(r_{ij})$ is the Jastrow pair function chosen to approximate the solution of two-body Schrödinger equation. The lattice is assumed to be triangular since this minimizes the potential energy [77]. The Jastrow function contains parameters which along with c are varied to minimize $E(p)$. For the liquid phases $c = 0$ but for a solid c takes a finite value treated as an adjustable parameter. Once a right choice of variational function is obtained, the ground state energy is further calculated using the DMC method. Starting with the imaginary time Schrödinger equation,

$$-\frac{\partial \psi(R, t)}{\partial t} = (H - E_T)\psi(R, t) \quad (1.45)$$

and by introducing $f(R, T) = \phi_T(R)\psi(R, t)$ as the mixed distribution function to the equation above we can obtain the diffusion-reaction equation [74],

$$\frac{\partial f}{\partial t} = \Lambda \sum_i \nabla_i^2 f - 2\Lambda^2 \sum_i \nabla_i \cdot (f \nabla_i \phi_T) - (E_L - E_T)f \quad (1.46)$$

where Λ is the dimensionless DeBoer parameter defined as $\Lambda = \hbar^2/2m\sigma^2\epsilon$ in which σ and ϵ are the reduced unit length and energy. $E_L = H\phi_T/\phi_T$ found in the last term represents the upper bound on the ground state energy. The value of E_T that gives a steady population is the exact ground state energy. Other properties such as the pair distribution functions are also calculated from the mixed distribution, $\phi_T(R)\psi_0(R)$ where $\psi_0(R)$ being the ground state in a large time evolution. The pair-correlation function $g(r)$ and the structure function $S(k)$ encode the information on the degree of order of the system. Oscillating pair-correlation function is what one anticipates when the system is in solid phase while a non-oscillating one signatures a liquid phase.

1.5 Brief outline of the thesis

The microscopic formalism developed in the first part of this thesis can accurately treat a weakly interacting Bose-Einstein condensate and a non-condensed thermal atoms for a range of temperatures below the 2D critical transition temperature T_c . In the same spirit, I assume the semi-classical Two-fluid model to be valid in evaluating the equilibrium property of the condensate fraction and the density profile of bosonic gas in this limit. In this model the density profiles are calculated self-consistently by ensuring that the choice of effective interaction potential is introduced in a consistent manner. It is an extremely important point since the introduction of inaccurate effective potential costs heavily in the convergence of the numerical solution. Another crucial fact to consider is the scattering property of a strictly 2D Bose gas, where the s -wave scattering length has become larger than the axial thickness of the cloud changes dramatically. In Sec. 2.1 I will illustrate how a semi-analytical expression for the many-body T-matrix elements corresponding to the condensate-condensate and to the condensate-thermal cloud coupling parameters (g_2 and g_1 , respectively) effects the equilibrium properties of the Two-fluid model at increasing temperature.

Sec. 2.2 summarizes the Feshbach formalism framework with application to the 2D Bose gas. Here I examine the tuning of two-body collisions by means of a magnetic field in a strictly 2D condensate inside a harmonic trap at zero temperature. By modifying the coupling strength one can control the dimensionless physical parameter η which is the ratio between the mean-field interaction energy and the harmonic-oscillator level spacing [41]. In the case of repulsive interactions ($\eta > 0$), starting from a weakly interacting regime ($\eta \ll 1$) and up to a strongly interacting one ($\eta \gg 1$), I evaluate the equilibrium density profile as a function of η by solving numerically a non-linear Schrödinger equation by a split-step Crank-Nicholson discretization scheme. In the case of attractive interactions ($\eta < 0$) one can give an upper bound for the number of bosons which can condense without the condensate

collapsing. At variance from the 3D gas (see for instance [49, 44]), I have found that in 2D this critical number does not depend explicitly on the strength of the harmonic confinement.

In Sec. 3.1, I consider a 2D rotating condensate at finite temperature and evaluate the particle density profiles and the energy of a vortex within a strictly 2D model for the boson-boson coupling. This is appropriate to a situation in which the s -wave scattering length starts to exceed the vertical confinement length. Previous work has established that the dimensionality of the scattering collisions strongly affects the equilibrium density profiles [78, 79] and the process of free expansion of a BEC containing a vortex [80]. A similar study of the density profiles of a rotating BEC in 3D geometry at finite temperature has been carried out by Mizushima *et al.* [81], who also determined the location of various dynamical instabilities within the Bogoliubov-Popov theory.

In Sec. 3.2, I will report the result of my investigation on the ground state properties of N_v vortices treated as N Yukawa bosons trapped in the two-dimensional harmonic trap. A density functional theory (DFT) approach is developed to calculate the density profiles and the ground state energy of the vortex fluid within the Bogoliubov-de Gennes reference system. When a non-interacting auxiliary system is inferred in this model, we obtained a Kohn-Sham (KS) type equation. As a preliminary step, the density profile of the vortex fluid is calculated by solving this equation numerically. The method relies on the VMC data of Magro and Ceperley [74] on the homogeneous ground state energies. The work in this thesis also pave way to many unresolved open questions pertaining to the physics of freezing and that of the strongly correlated incompressible liquid which has an overlap with the Fractional Quantum Hall Effect (FQHE).

Chapter 2

Scattering properties for 2D Bose gas

2.1 Coupling parameters in a mixture of condensed and thermal-bosons

The scattering property of bosons in a 2D flat geometry changes dramatically compared to the 3D one. The T-matrix for two-body collisions *in vacuo* at low momenta and energy, which should be used to obtain the collisional coupling parameter to the lowest order in the particle density, vanishes in the strictly 2D limit [12, 40]. It is then necessary to evaluate the scattering processes between pairs of Bose particles by taking into account the presence of a condensate and a thermal cloud through a many-body T-matrix formalism [82, 83, 84].

This formalism has already been used in a number of studies of low dimensional Bose gases, dealing in particular with phase fluctuations and the Kosterlitz-Thouless transition in a variational approach [82, 83, 37, 85], with a mean-field evaluation of the breathing-mode frequency in a trapped 1D gas [86], and with the equilibrium density profile of a 2D condensate [84, 78]. In the limit of zero temperature the condensate-condensate coupling parameter has been related to the two-body T-matrix by considering that, when two

particles in the condensate collide at zero momentum, they both require an energy equal to the chemical potential μ to be excited out of the condensate [84]. With increasing temperature the population of the excited states becomes non-negligible and a microscopic theory which also takes into account the depletion of the condensate is required [87]. An additional coupling parameter to describe the scattering processes between an atom in the condensate and an atom in the thermal cloud has been introduced by Stoof and co-workers [37] through the two-body T-matrix at energy $-\mu$.

The scattering processes between pairs of atoms in a gas consisting of a Bose-Einstein condensate cloud and a thermal cloud are described by the many-body T-matrix $T^{MB}(E)$ as a function of the energy E . The coupling parameters are given by the matrix elements $\langle \mathbf{k}' | T^{MB}(E) | \mathbf{k} \rangle \equiv T^{MB}(\mathbf{k}, \mathbf{k}', \mathbf{K}; E)$, taken in the limit of zero energy and momenta. Here \mathbf{k} and \mathbf{k}' are the incoming and outgoing relative momenta of the pair of center-of-mass momentum \mathbf{K} . I will consider only the condensate-condensate and condensate-thermal cloud couplings and neglect the scattering between thermally excited atoms in the present case of a dilute gas.

Before discussing the many-body T-matrix, however, we shall first recall the behaviour of the two-body T-matrix that describes collisions between pairs of particles *in vacuo*. We shall then discuss how the two T-matrices are related in the appropriate limit for a two-fluid system.

2.1.1 The two-body T-matrix

The two-body T-matrix is the solution of the Lippmann-Schwinger equation,

$$\begin{aligned} \langle \mathbf{k}' | T^{2B}(\bar{E}) | \mathbf{k} \rangle &= \langle \mathbf{k}' | V(|\mathbf{r}_1 - \mathbf{r}_2|) | \mathbf{k} \rangle + \sum_{\mathbf{q}} \langle \mathbf{k}' | V(|\mathbf{r}_1 - \mathbf{r}_2|) | \mathbf{q} \rangle \\ &\times \frac{1}{\bar{E} - 2\epsilon_{\mathbf{q}}} \langle \mathbf{q} | T^{2B}(\bar{E}) | \mathbf{k} \rangle, \end{aligned} \quad (2.1)$$

with $V(|\mathbf{r}_1 - \mathbf{r}_2|)$ being the interparticle potential. The center-of-mass energy for the pair of atoms is \bar{E} and each atom of mass m has a single-particle

excitation energy $\epsilon_{\mathbf{q}} = \hbar^2 q^2 / 2m$, as the collision takes place in free space. In Eq. (2.1) the collisions are described by a single-loop interaction between the two atoms plus contributions involving all possible transition routes from state $|\mathbf{k}\rangle$ to state $|\mathbf{k}'\rangle$ via intermediate states $|\mathbf{q}\rangle$.

In the case of the hard-disk potential of strength $V_0 = 4\pi\hbar^2/m$ and in the dilute limit ($\mathbf{k}a, \mathbf{k}'a \ll 1$), the solution of Eq. (2.1) is [37]

$$\langle \mathbf{k}' | T^{2B}(\bar{E}) | \mathbf{k} \rangle \approx \frac{4\pi\hbar^2/m}{\ln |4\hbar^2/\bar{E}ma^2|}. \quad (2.2)$$

In this case the T-matrix is independent of the momenta, but depends on the logarithm of the energy and vanishes as \bar{E} approaches zero. Therefore, the presence of the surrounding gas must be taken into account in the collisional processes. Following the proposal of Morgan et al. [88], this is done by setting $\bar{E} = -2\mu$ for the mutual scattering of two condensate particles, this being the energy required for them to be excited out of the condensate. By a similar argument Al Khawaja et al. [37] set $\bar{E} = -\mu$ for the scattering between a boson in the condensate and boson in the thermal cloud.

2.1.2 The many-body T-matrix

According to the above argument, a first approximation for the many-body T-matrix at zero momenta and energy is

$$T_n^{MB}(0, 0, 0; 0) = T^{2B}(0, 0, 0; -n\mu) \quad (2.3)$$

with $n = 1$ for condensate-thermal cloud scattering and $n = 2$ for condensate-condensate scattering. Further many-body effects can enter the scattering processes attended by the presence of a condensate from attributing a Bogoliubov spectrum to the intermediate states [82]. At low momenta the many-body T-matrix is the solution of the integral equation

$$\begin{aligned} \langle \mathbf{k}' | T^{MB}(E) | \mathbf{k} \rangle &= \langle \mathbf{k}' | V(|\mathbf{r}_1 - \mathbf{r}_2|) | \mathbf{k} \rangle + \sum_{\mathbf{q}} \langle \mathbf{k}' | \mathbf{V}(|\mathbf{r}_1 - \mathbf{r}_2|) | \mathbf{q} \rangle \\ &\times \frac{1 + 2N(\omega_{\mathbf{q}})}{E - 2\hbar\omega_{\mathbf{q}}} \langle \mathbf{q} | T^{MB}(E) | \mathbf{k} \rangle \end{aligned} \quad (2.4)$$

where $\hbar\omega_{\mathbf{q}} \approx \epsilon_{\mathbf{q}} + \mu$ are the Bogoliubov excitation energies in the Hartree approximation $\mu \ll \epsilon_{\mathbf{q}}$ and $N(\omega_{\mathbf{q}}) \approx \exp[\beta(\epsilon_{\mathbf{q}} + \mu)] - 1^{-1}$ are the corresponding population factors. For a contact interaction potential of Eq. (2.4) yields

$$T^{MB}(0, 0, 0; E) = \left[\frac{1}{V_0} - \sum_{\mathbf{q}} \frac{1 + 2N(\omega_{\mathbf{q}})}{E - 2\hbar\omega_{\mathbf{q}}} \right]^{-1}. \quad (2.5)$$

As discussed by Stoof and Bijlsma [82, 83]. Eq. (2.5) is still affected by an ultraviolet divergence, which can be remedied by replacing V_0 in favor of the two-body T-matrix. The final result is

$$T_n^{MB}(0, 0, 0; 0) = T^{2B}(0, 0, 0; -n\mu) \left[1 + T^{2B}(0, 0, 0; -n\mu) \sum_{\mathbf{q}} \frac{N(\omega_{\mathbf{q}})}{\hbar\omega_{\mathbf{q}}} \right]^{-1}, \quad (2.6)$$

with $T^{2B}(0, 0, 0; -n\mu)$ given by Eq.(2.2) with $\bar{E} = -n\mu$.

2.1.3 Calculation of coupling parameters

The sum in the RHS of Eq.(2.6) can be evaluated analytically by replacing the sum over intermediate states by an integral over momentum. Setting $N(\omega_{\mathbf{q}}) = \sum_{s=1}^{\infty} \exp(-s\beta\hbar\omega_{\mathbf{q}})$, we get

$$\sum_{\mathbf{q}} \frac{N(\omega_{\mathbf{q}})}{\hbar\omega_{\mathbf{q}}} = -\frac{m}{2\pi\hbar^2} \sum_{s=1}^{\infty} Ei(-s\beta\mu) \quad (2.7)$$

where $Ei(x)$ is the exponent-integral function. In the asymptotic low-temperature regime ($\beta\mu \gg 1$) this thermal-population term can be approximated by

$$\sum_{s=1}^{\infty} Ei(-s\beta\mu) \rightarrow (\beta\mu)^{-1} \ln[1 - \exp(-\beta\mu)]. \quad (2.8)$$

A numerical illustration is given in Fig. (2.1) for values of the system parameters appropriate to the experiments on ^{23}Na by Görlitz *et al.* [17] (see Sec. (2.1.4)).

In summary, the coupling parameters in the 2D Bose gas are given by

$$g_n^{MB} = \frac{4\pi\hbar^2/m}{\ln |4\hbar^2/(nm\mu a^2)| - 2 \sum_{s=1}^{\infty} Ei(-s\beta\mu)}, \quad (2.9)$$

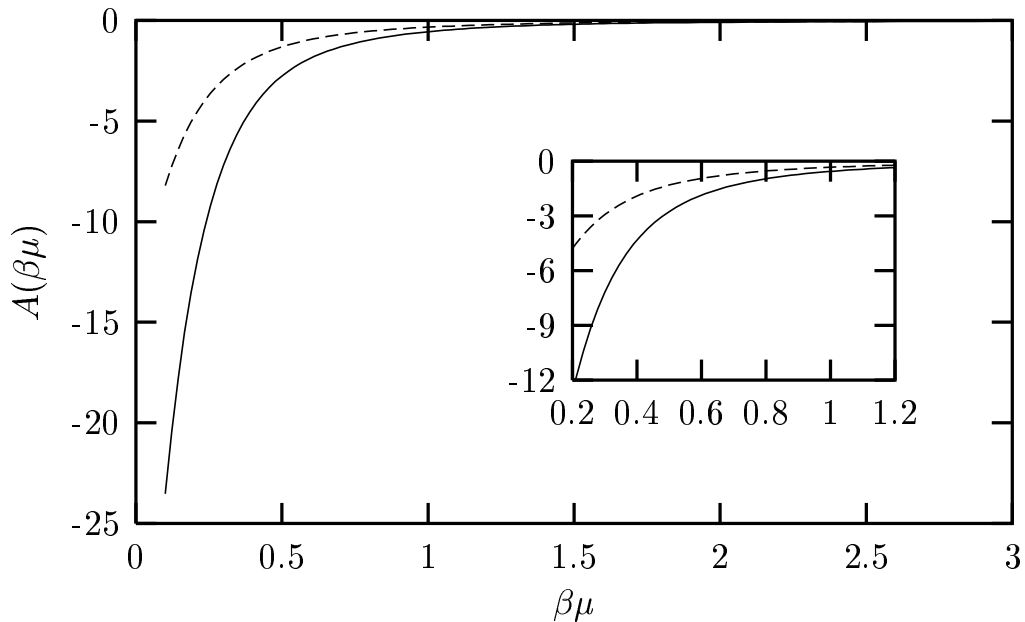


Figure 2.1: The correction term $A(\beta\mu)=\sum_{s=1}^{\infty} Ei(-s\beta\mu)$ from excited-state occupancy (dashed line) and its approximate form Eq. (2.8) (solid line) as functions of $\beta\mu$. In the inset a zoom of the region $0.2 < \beta\mu < 1.2$ is shown.

with $n=2$ for collision between pairs of condensate atoms and $n=1$ for collisions between an atom in the condensate and thermally excited atom. These parameters depend on temperature both through the chemical potential and through the excited-state population factor given in Eq. (2.7) and asymptotically approximated by Eq.(2.8). If this population factor is dropped, one obtains from Eq.(2.3) the corresponding “two-body” coupling parameters as

$$g_n^{2B} = \frac{4\pi\hbar^2/m}{\ln|4\hbar^2/(nm\mu a^2)|}. \quad (2.10)$$

In the next Section I evaluate the chemical potential and hence the coupling parameters in Eqs. (2.9) and (2.10) through a self-consistent evaluation of the density profiles in a two fluid-model.

2.1.4 Equilibrium properties in the two-fluid model

Let $n_c(r)$ and $n_{nc}(r)$ be the particle density profiles for the condensate and for the thermal cloud in a 2D Bose gas which is radially confined inside a isotropic planar trap described by the external potential $V_{ext}(r) = \frac{m\omega_{\perp}^2 r^2}{2}$. The two-fluid model [36, 89] combines a solution of the Gross-Pitaevskii equation for the condensate with a Hartree-Fock model of the thermal cloud, which is treated as an ideal gas subject to an effective potential $V_{eff}(r)$. In the present case,

$$V_{eff}(r) = V_{ext}(r) + 2g_1 n_c. \quad (2.11)$$

As already noted, we are neglecting the collisions between pairs of bosons belonging to the thermal cloud.

It is well known that a full numerical solution of the Gross-Pitaevskii equation Eq. (1.28) can be avoided when the kinetic energy term in it can be neglected [46]. I postpone the evaluation of a full scale numerical solution of the GPE equation for the coming Sec. (2.2) on Feshbach resonances and in chapter 3, where the role of the kinetic energy become crucial in vortex calculation. Since our goal here is to analyse the effect of the interactions on the equilibrium properties of the system, we use the Thomas-Fermi approximation in which kinetic energy is neglected. This yields a condensate density of the form

$$n_c(r) = (1/g_2)[\mu - V_{ext}(r) - 2g_1 n_{nc}(r)]\theta(\mu - V_{ext}(r) - 2g_1 n_{nc}(r)). \quad (2.12)$$

where $\theta(x) = 0$ for $x < 0$ otherwise $\theta(x) = 1$ if $x > 0$. Since I am interested in examining qualitative behaviours rather than in attaining high numerical accuracy, I have adopted Eq.(2.12) for the condensate density and found that discontinuities occurring in the density profiles at the Thomas-Fermi radius can be eliminated by the simple expedient of introducing a momentum cut-off in the expression for $n_{nc}(r)$ of Eq. (1.30). That is, we calculate $n_{nc}(r)$ from

$$n_{nc}(r) = -\frac{m}{2\pi\hbar^2\beta} \ln \left[1 - \exp\left[\beta\left(\mu - V_{eff}(r) - \frac{p_0^2}{m}\right)\right] \right], \quad (2.13)$$

where we take $p_0 = \sqrt{mg_1 n_{nc}}$ [90]. The model is then evaluated by solving self-consistently Eqs. (2.11)-(2.13) together with the condition that the areal integral of $n_c(r)+n_{nc}(r)$ should be equal to the total number N of particles.

The validity of the present model is as follows. A mean-field treatment is valid when the diluteness condition $n_c a^2 \ll 1$ holds and if the temperature of the gas is outside the critical region. With regard to the thermal cloud, no significant differences have been found between the predictions of the Hartree-Fock and Popov approximations in the regime $n_c a^2 \ll 1$, except at very low temperature where the thermal cloud is becoming negligible [91].

2.1.5 Coupling strength and its effect on equilibrium properties

For a numerical illustration, we have taken the values of particle number, the radial trap frequency, and the scattering length as appropriate for ^{23}Na atoms in the experiment of Görlitz *et al.*[17] ($N = 5 \times 10^5$, $\omega_{\perp} = 188.4$ Hz, $a = 2.8$ nm). Whereas in their experiment collisions are in 3D regime, we focus on a strictly 2D regime that could be reached experimentally by increasing either the trap anisotropy parameter or the scattering length.

I have compared the temperature dependence of the coupling parameters g_n^{2B} (long dashes for $n=2$ and short dashes for $n=1$) with that of the coupling parameters g_n^{MB} (full and dotted lines, respectively) in Fig. (2.2). It is evident that the many-body screening of the interactions due to the occupancy of excited states is quite large and rapidly increasing with temperature.

Such many-body screening has, however, very little effect on equilibrium properties of the gas for our choice of system parameters. Figure (2.3) reports the condensate fraction N_0/N for the g_n^M model as a function of temperature, in comparison with that of an ideal Bose gas at the same values of the system parameters. As is well known, the transition temperature and the condensate fraction are lowered by the interactions. However, the g_n^{2B} model gives results that are practically the same as the g_n^{MB} one.

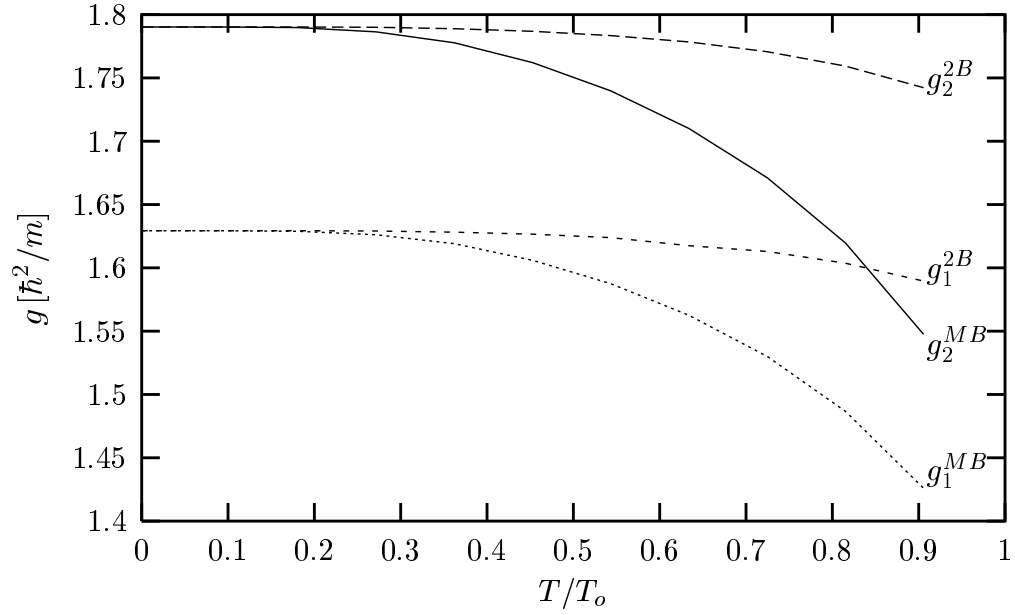


Figure 2.2: Interaction strengths (in units of \hbar^2/m) as functions of temperature T (in units of ideal-gas critical temperature T_0).

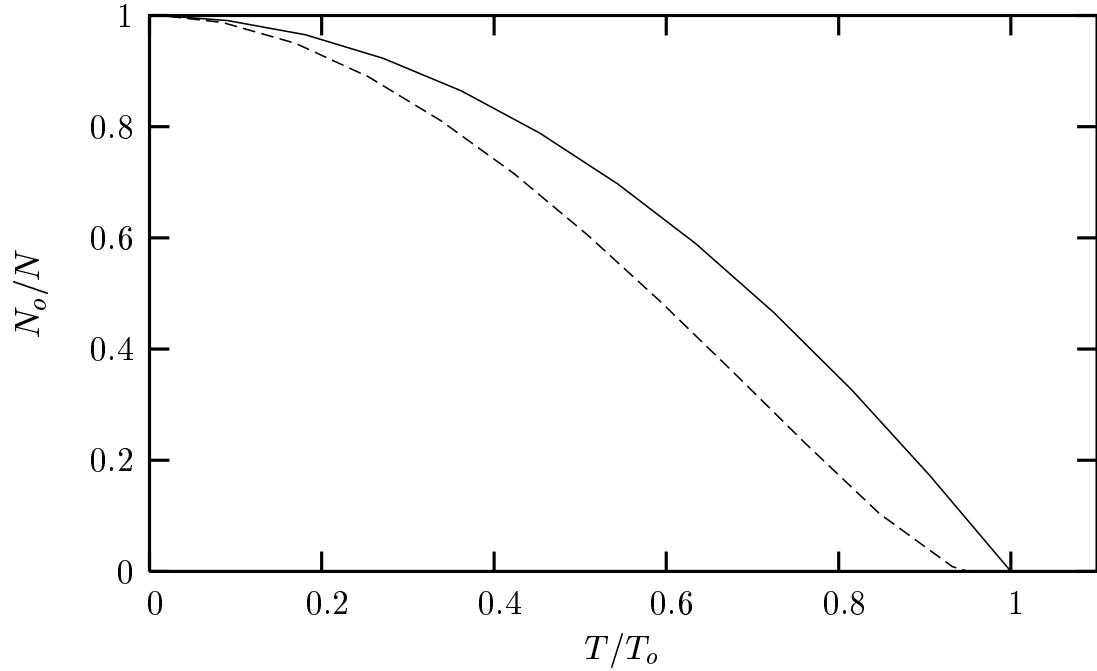


Figure 2.3: Condensate fraction N_0/N as a function of temperature T (in units of T_0) from the g_n^{MB} model and (dashed line) compared with the non-interacting gas (solid line).

The evolution of the density profiles for the condensate and for the thermal cloud with increasing temperature from near absolute zero to the critical temperature T_0 of the ideal gas ($T_0 = (\sqrt{6}/\pi)\hbar\omega\sqrt{N}$ [92]) are depicted in Figure (2.4). The results in Figure (2.4a) are in good agreement with those of Tanatar et al. [78], except that the tails of that profile are missed in the Thomas-Fermi approximation. Again the screening of collision from the occupancy of the excited states is very small and becomes barely visible at $T \approx 0.75 T_0$.

We can deduce that the use of Eq. (2.3) to describe the many-body effects in two-body scattering processes in 2D Bose-condensed gas appears to be very good in regard to equilibrium properties at large values of the particle number. A decrease in the number of particles lowers the chemical potential and may lead to observable effects for $N \approx 10^3$.

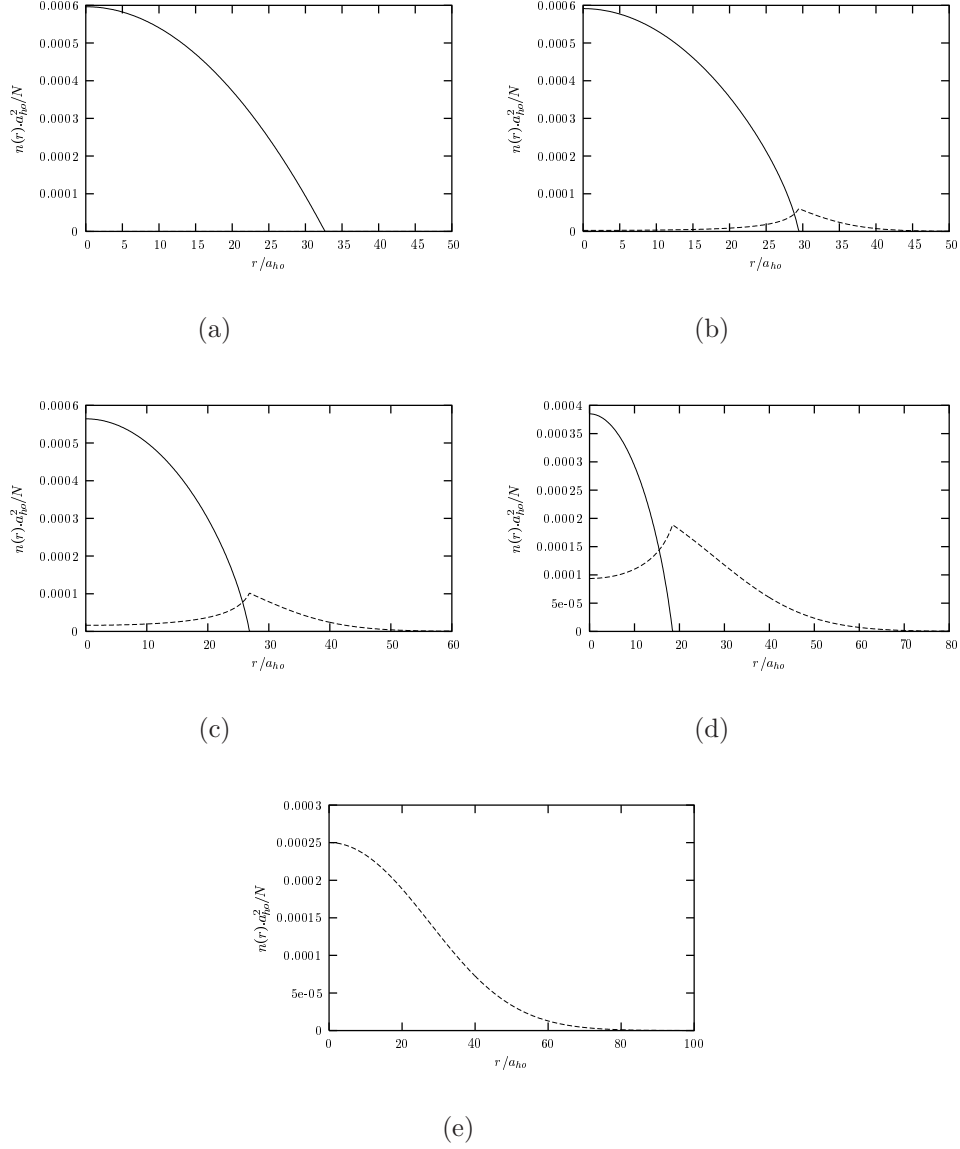


Figure 2.4: Density profiles of the condensate (solid line) and the thermal cloud (dashed line) in the g_n^{MB} model (in units of N/a_{ho}^2 with $a_{ho} = (\hbar/m\omega)^{1/2}$) as functions of radial distance r (in units of a_{ho}) at various values of the temperature ($T/T_0=0,0.3,0.5,0.8$ and 0.95 from (a) to (e)).

2.2 Feshbach resonance in a 2D Bose gas

The 3D s -wave scattering length can be tuned by means of external electric or magnetic fields [93, 39, 94]. Within this process a resonance can appear at a particular value of the magnetic field and allows control of the coupling strength ranging from positive (repulsive) to negative (attractive) values. One may study new dynamical effects of collective oscillations in large condensates [95] and the dynamics of collapsing and exploding condensates [96]. Calculations of such Feshbach resonances have been given for 3D gases of ^7Li [97], ^{23}Na [39], ^{39}K and ^{41}K [98], ^{85}Rb and ^{87}Rb [94], and ^{133}Cs [93]. Experimental observations have been reported for ^{87}Rb [99], ^{85}Rb [96, 100, 101, 102], ^{23}Na [103], and ^{133}Cs [104]. Feshbach resonances in quasi-2D atomic gases have been discussed by Wouters *et al.* [105], who have predicted a shift in the position of the resonance from the squeezing of the confinement.

2.2.1 Overview on scattering theory

We start by recalling some well-known facts about a collision between two particles with internal degrees of freedom governed by an internal Hamiltonian H^{int} ,

$$H^{int} |\alpha\rangle = \epsilon_\alpha |\alpha\rangle \quad (2.14)$$

where $|\alpha\rangle$ and ϵ_α are the single-atom eigenstate and its corresponding eigenvalue. For example the internal Hamiltonian can describe the hyperfine interaction between nuclear and electronic spins and their Zeeman coupling to an external magnetic field B . A two-body collision is described by the Hamiltonian

$$H = \frac{p^2}{2m_r} + \sum_{i=1}^2 H_i^{int} + V(\mathbf{r}) \quad (2.15)$$

in the center-of-mass system, with \mathbf{p} the relative momentum and m_r the reduced mass (see for instance [106]). The Hamiltonian in Eq. (2.15) is the sum of a part with eigenstates $|\alpha\beta\rangle$ (“channels”) tending asymptotically to a symmetrized product of separate-atom internal states $|\alpha\rangle$ and $|\beta\rangle$, and

of a finite-range interaction $V(\mathbf{r})$ which couples the channels. The energy associated with an eigenstate $|\alpha\beta\rangle$ is $E_{\alpha\beta} = \varepsilon_\alpha + \varepsilon_\beta + \hbar^2 k_{\alpha,\beta}^2 / 2m_r$, where $\hbar\mathbf{k}_{\alpha,\beta}$ is the relative momentum of the two incoming particles. The asymptotic scattering state $\Psi_{\alpha\beta}(\mathbf{r})$ can be expanded on all scattering channels in the form

$$\Psi_{\alpha\beta}(\mathbf{r}) = \exp(i\mathbf{k}_{\alpha\beta} \cdot \mathbf{r}) |\alpha\beta\rangle + \sum_{\alpha',\beta'} f_{\alpha\beta}^{\alpha'\beta'}(\mathbf{k}_{\alpha\beta}, \mathbf{k}'_{\alpha'\beta'}) \frac{\exp(i\mathbf{k}'_{\alpha'\beta'} \cdot \mathbf{r})}{r} |\alpha'\beta'\rangle, \quad (2.16)$$

where the outgoing channel is denoted by $|\alpha'\beta'\rangle$ and the scattering amplitude $f_{\alpha\beta}^{\alpha'\beta'}$ is proportional to the T-matrix element $\langle \mathbf{k}'_{\alpha'\beta'} | T | \mathbf{k}_{\alpha\beta} \rangle$. The asymptotic magnitude of the momentum for the $|\alpha'\beta'\rangle$ channel is $k_{\alpha'\beta'} = \sqrt{2m_r(E_{\alpha\beta} - \varepsilon_{\alpha'} - \varepsilon_{\beta'})}$, from conservation of total momentum and energy in the scattering process. The channel is said to be open (closed) if the momentum takes positive real (imaginary) value.

The whole Hilbert space describing the spatial and spin degrees of freedom is now divided into a subspace P for open channels and a subspace Q including all closed channels [107]. The state vector $|\Psi\rangle$ and the Schrödinger equation $H|\Psi\rangle = E|\Psi\rangle$ are projected onto the two subspaces by means of projection operators P and Q satisfying the conditions $P + Q = 1$ and $PQ = 0$. The formal solution of the coupled equations obeyed by the two projected components is

$$|\Psi_Q\rangle = (E - H_{QQ} + i\delta)^{-1} H_{QP} |\Psi_P\rangle \quad (2.17)$$

and

$$(E - H_{PP} - H'_{PP}) |\Psi_P\rangle = 0, \quad (2.18)$$

where $H_{PP} = PHP$ etc.,

$$H'_{PP} = H_{PQ}(E - H_{QQ} + i\delta)^{-1} H_{QP}, \quad (2.19)$$

and δ is a positive infinitesimal. The term H'_{PP} in Eq. (2.18) describes the Feshbach resonances. It represents an effective non-local, retarded interaction in the P subspace due to transitions to the Q subspace and back. The

Hamiltonian $H_{PP} + H'_{PP}$ gives the effective atom-atom interaction in the open-channel subspace, the effects due to the existence of bound states being taken into account through the term H'_{PP} .

2.2.2 Feshbach resonances in the 2D coupling

A Feshbach resonance results when true bound states belonging to the closed-channel subspace match the energy of open channels: transient transitions may then be possible during the collision process [39]. Setting $H_{PP} = H_0 + U_1$ where H_0 includes the kinetic energy of relative motion and the internal Hamiltonian, the scattering matrix elements in the P subspace between plane-wave states with relative momenta \mathbf{k} and \mathbf{k}' read

$$\langle \mathbf{k}' | T | \mathbf{k} \rangle \simeq \langle \mathbf{k}' | T_1 | \mathbf{k} \rangle + \langle \Omega_{1,+} \mathbf{k}' | H'_{PP} | \Omega_{1,+} \mathbf{k} \rangle . \quad (2.20)$$

Here $T_1 = U_1 + U_1 G_0 T_1$ represents the scattering process if Q subspace is neglected and $\Omega_{1,+} = (1 - G_0 U_1)^{-1}$ is the wave operator due to the interaction potential U_1 , with $G_0 = (E - H_0)^{-1}$ [8]. In Eq. (2.20) the effect of closed channels has been included at first order in H'_{PP} . In the limit of zero relative velocity Eq. (2.20) leads to an expression for the coupling strength,

$$g = \tilde{g} + \sum_n \frac{|\langle \psi_n | H_{QP} | \psi_0 \rangle|^2}{E_{th} - E_n} \quad (2.21)$$

where the sum is over all the states $|\psi_n\rangle$ in Q subspace and we have set $|\Omega_{1,+} \mathbf{k}\rangle \simeq |\Omega_{1,+} \mathbf{k}'\rangle \equiv |\psi_0\rangle$. Here, \tilde{g} is the coupling strength estimated in the absence of closed channels and E_{th} is the threshold energy for the state $|\psi_0\rangle$ at vanishing kinetic energy. Finally, when the threshold energy is close to the energy E_{res} of one specific bound state $|\psi_{res}\rangle$, this contribution will be dominant and the contributions from all other states may be included in \tilde{g} through an effective non-resonant scattering length a_{nr} . For a strictly 2D condensate we get

$$g = \frac{4\pi\hbar^2/m}{\ln |4\hbar/\mu m a_{nr}^2|} + \frac{|\langle \psi_{res} | H_{QP} | \psi_0 \rangle|^2}{E_{th} - E_{res}}, \quad (2.22)$$

where μ is the chemical potential of the condensate. Equation (2.22) is our main result. The non-resonant first term has been calculated from the two-body T-matrix for a binary collision occurring at low momenta and energy in the presence of a condensate, which fixes the energy of each colliding atom at the chemical potential [88, 79]. The resonant second term can be tuned by exploiting the dependence of the energy denominator on external parameters and in particular on the strength of the applied magnetic field. Explicitly, if the energy denominator vanishes at a value B_0 of the field, then by expansion around this value we have

$$E_{th} - E_{res} \approx (\mathbf{m}_{res} - \mathbf{m}_\alpha - \mathbf{m}_\beta)(B - B_0) \quad (2.23)$$

where $\mathbf{m}_{\alpha,\beta} = -\partial\epsilon_{\alpha,\beta}/\partial B$ are the magnetic moments of the two colliding atoms in the open channel and $\mathbf{m}_{res} = -\partial E_{res}/\partial B$ is the magnetic moment of the molecular bound state. Equation (2.22) then yields

$$g = \frac{4\pi\hbar^2}{m} \left(\frac{1}{\ln|4\hbar/\mu m a_{nr}^2|} + \frac{\Delta B}{B - B_0} \right), \quad (2.24)$$

where the width parameter ΔB is defined as

$$\Delta B = \frac{m}{4\pi\hbar^2} \frac{|\langle\psi_{res}|H_{QP}|\psi_0\rangle|^2}{\mathbf{m}_{res} - \mathbf{m}_\alpha - \mathbf{m}_\beta}. \quad (2.25)$$

Higher-order terms in H'_{PP} will lead to a broadening of the resonance. However, the width of resonant states close to the threshold energy in the open channel is usually small because of the low density of states, and Feshbach resonances are usually very sharp [8].

In the next Section I will analyze the consequences of tuning the coupling strength on the equilibrium state of a 2D condensate in a harmonic trap.

2.2.3 Equilibrium properties as functions of the coupling

We consider a Bose gas with a fixed number N of particles in a 2D harmonic potential $V_{ext}(r) = m\omega^2 r^2/2$. At zero temperature the condensate wave

function $\Psi(r)$ is described by the mean-field Gross-Pitaevskii equation

$$\left[-\frac{\hbar^2}{2m} \frac{1}{r} \frac{\partial}{\partial r} \left(r \frac{\partial}{\partial r} \right) + V_{ext}(r) + gn_c(r) \right] \Psi(r) = \mu \Psi(r), \quad (2.26)$$

where $n_c(r) = |\Psi(r)|^2$ is the density of the condensate. We introduce the dimensionless coordinate $x = r/a_{ho}$, where $a_{ho} = (\hbar/m\omega)^{1/2}$ is the harmonic oscillator length, and the dimensionless chemical potential $\mu' = 2\mu/\hbar\omega$. Thus Eq. (2.26) can be written in rescaled form as

$$\left[-\frac{d^2}{dx^2} - \frac{1}{x} \frac{d}{dx} \right] \Psi(x) + x^2 \Psi(x) + 2\eta \left| \frac{\Psi(x)}{\Psi(0)} \right|^2 \Psi(x) = \mu' \Psi(x), \quad (2.27)$$

where $\eta = g|\Psi(0)|^2/\hbar\omega$ is a dimensionless coupling parameter given by the ratio between the mean-field interaction energy per particle and the oscillator level spacing. The normalization condition on the wave-function is

$$N = a_{ho}^2 \int_0^\infty x dx |\Psi(x)|^2. \quad (2.28)$$

Equations (2.27) and (2.28) need to be solved self-consistently.

2.2.4 Repulsive coupling ($\eta > 0$)

In the case of repulsive interactions Eq. (2.27) always admits a solution: the condensate exists and is stable in the 2D harmonic trap. Of course, far away from the resonance the dimensionless coupling parameter η is primarily determined by the non-resonant scattering length. On approaching the resonance by increasing B towards B_0 , the coupling parameter becomes very small for $B \sim B_0 - \Delta B / (\ln |4\hbar/\mu m a_{nr}^2|)$: the non-linear term in Eq. (2.27) becomes small and the condensate wave function is close to a Gaussian profile. On further increasing B the gas enters the strong-coupling regime and in the limit $\eta \gg 1$ the kinetic energy term in Eq. (2.27) and the discrete structure of the trap levels become irrelevant. The profile then approaches a Thomas-Fermi form [33, 45]. The shape of the condensate density profile, obtained by the numerical solution of Eq. (2.27) at several values of

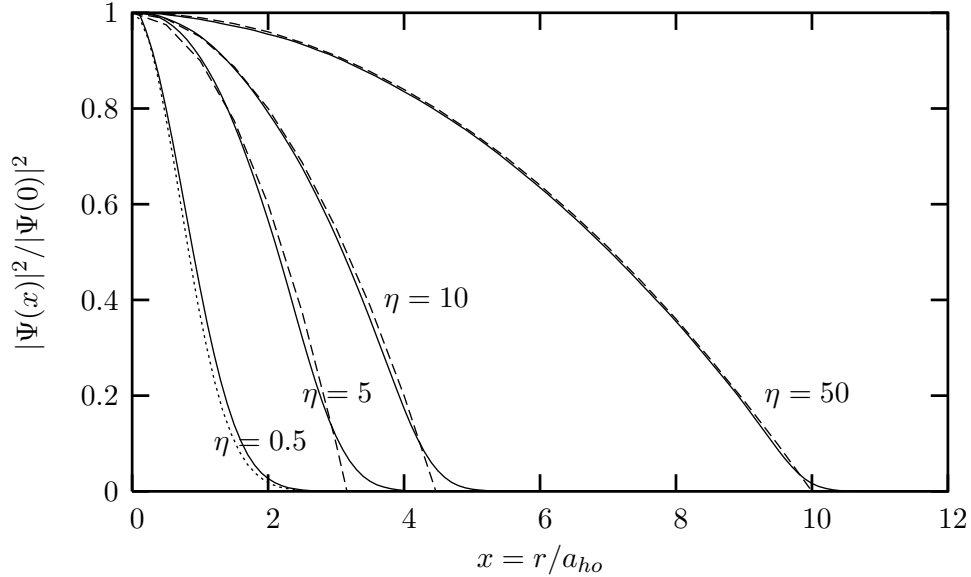


Figure 2.5: Scaled density profile $|\Psi(x)|^2/|\Psi(0)|^2$ as a function of the dimensionless radial distance $x = r/a_{ho}$ for various values of the coupling parameter η . Dashed curves are Thomas-Fermi profiles and the dotted curve is the free-gas profile.

the coupling parameter η , is depicted in Fig. 2.5. The Figure illustrates comparisons with the free-gas and Thomas-Fermi profiles, according to the discussion given just above.

2.2.5 Attractive coupling ($\eta < 0$)

On going through the resonance the Thomas-Fermi-like density profile will suddenly shrink and collapse. Indeed, in the strong-coupling attractive regime the kinetic energy does not suffice to compensate for the negative mean-field energy term and Eq. (2.26) does not admit physical solutions. A condensate with a limited number of particles can only exist in the weakly attractive regime. An upper bound for the critical number N_c of bosons in a condensate with weakly attractive interactions can be estimated by comparing the kinetic energy and the mean-field energy at the centre of the trap. This leads

to the inequality

$$1 + 2\eta \geq 0 \tag{2.29}$$

for condensate stability, where in the calculation of the kinetic energy we have used the free-gas wave function. Using the expression of η we find from Eq. (2.29)

$$N_c \simeq \left| \frac{1}{\ln |4\hbar/\mu m a_{rr}^2|} + \frac{\Delta B}{B - B_0} \right|^{-1}. \tag{2.30}$$

At variance from the trapped 3D gas [49], the critical number N_c does not depend on the harmonic oscillator length, the dependence being cancelled by the fact that in 2D the mean-field energy scales as $\approx a_{ho}^{-2}$ like the kinetic energy. Let us remark that the condensate in the case of attractive coupling can be metastable even if the number of condensed bosons is lower than N_c . A three-body loss term should be included in Eq. (2.26) in order to calculate the decay time and to describe the time evolution of such a condensate, as was done for the 3D Bose gas [44, 42, 43] and very recently for a 3D boson-fermion mixture [108]. An evaluation of three-body losses in the 2D Bose gas and of the time evolution of a 2D condensate in the weakly attractive coupling regime may be considered in the future.

Chapter 3

Rotating 2D trapped Bose gas

3.1 Single vortex in a rotating 2D Bose gas

Understanding the behaviour of vortices in the 2D regime is important, since they reflect the superfluid nature of the condensate [109, 110, 91] and are expected to play a role in the transition from the superfluid to the normal state [16]. An experimental method for the creation of quantized vortices in a trapped BEC has made use of an "optical spoon" [54, 111], whereby the condensate in an elongated trap is set into rotation by stirring with laser beams. This experiment on a confined boson gas is conceptually the analogue of the rotating bucket experiment on bulk superfluid Helium, with the difference that the thermal cloud is inhomogeneously distributed and lies mostly outside the condensate cloud. A quantized vortex first appears in the condensate at a critical angular frequency of stirring which corresponds to an instability of the vortex-free state. A lower bound for the critical frequency can be assessed from the energy of a vortex, defined as the difference in the internal energy of the gas with and without a vortex. Observation of a vortex in a trapped gas is difficult since the vortex core is small in comparison to the size of the boson cloud, but the size of the core increases during free expansion and indeed vortices were first observed experimentally by releasing the trap and allowing ballistic expansion of the cloud [54].

3.1.1 GP model that accomodates a single vortex

The BEC is subject to an anisotropic harmonic confinement characterized by the radial trap frequency ω_{\perp} and by the axial frequency $\lambda\omega_{\perp}$ with $\lambda \gg 1$. Motions along the z direction are suppressed and the condensate wave function is determined by a 2D equation of motion in the $\{x, y\}$ plane.

The order parameter for a 2D condensate accommodating a quantized vortex state of angular momentum $\hbar\kappa$ per particle is written as $\Psi(\mathbf{r}) = \psi(r) \exp(i\kappa\phi)$, with ϕ the azimuthal angle. The wave function $\Psi(r)$ then obeys the nonlinear Schrödinger equation (NLSE)

$$\left[-\frac{\hbar^2}{2m} \nabla^2 + \frac{\hbar^2 \kappa^2}{2mr^2} + \frac{1}{2} m \omega_{\perp}^2 r^2 + g_2 n_c(r) + 2g_1 n_{nc}(r) \right] \Psi(r) = \mu \Psi(r) \quad (3.1)$$

similar to Eq. (1.28) but in addition it includes the contribution $2g_1 n_{nc}(r)$ of the thermal clouds. The 2D coupling parameters g_j , with $j = 2$ for condensate-condensate repulsions and $j = 1$ for condensate-noncondensate repulsions, are given by

$$g_j^{2B} = \frac{4\pi\hbar^2/m}{\ln |4\hbar^2/(jm\mu a^2)|}. \quad (3.2)$$

In Eq. (3.2) above we have omitted a term due to thermal excitations [79], which is negligible in the temperature range of present interest ($T \leq 0.5T_c$, with T_c the critical temperature).

In this model the atoms in the thermal cloud are not put directly into rotation, but feel the rotating condensate through the mean-field interactions. In the Hartree-Fock approximation [36] the thermal cloud is treated as an ideal gas subject to the effective potential $V_{eff}(r)$ written as in Eq. (2.11). The density distribution of the thermal cloud is then given by Eq. (2.13) in which the momentum cut-off p_0 in Eq. (2.13) is equivalent to adding the term $2g_1 n_{nc}$ to the effective potential in Eq. (2.11).

We solve self-consistently the coupled Eqs. (3.1) and (2.13) together with the condition that the areal integral of $n_c(r) + n_{nc}(r)$ is equal to the total

number N of particles. The differential equation (3.1) is solved iteratively by discretization, using a two-step Crank-Nicholson scheme [112]. In Sec. (3.1.3) I will also compare the results with those obtained in the Thomas-Fermi approximation by dropping the radial kinetic energy term in Eq. (3.1).

3.1.2 The energy of a vortex

The critical angular velocity measured in experiments where vortex nucleation occurs from a dynamical instability [54] depends strongly on the shape of the perturbation. However, a lower bound for the angular velocity required to produce a single-vortex state can be estimated once the energies of the states with and without the vortex are known. Since the angular momentum per particle is $\hbar\kappa$, the critical (thermodynamic) angular velocity is given by

$$\Omega_c = \frac{E_\kappa - E_{\kappa=0}}{N\hbar\kappa}. \quad (3.3)$$

This expression follows by equating the energy of the vortex state in the rotating frame, that is $E_\kappa - \Omega_c L_z$, to the energy $E_{\kappa=0}$ of the vortex-free state.

In the noninteracting case at zero temperature, the energy difference per particle is simply $\hbar\kappa\omega_\perp$, so that Ω_c is just the trap frequency in the $\{x, y\}$ plane. For the interacting gas at zero temperature in the Thomas-Fermi approximation, Eq. (3.3) reduces to the expression [46, 109]

$$\Omega_c^{TF}(0) = \frac{2\hbar}{mR^2} \ln \left(\frac{0.888 R}{\xi} \right). \quad (3.4)$$

Here $R = (2\mu/m\omega_\perp^2)^{1/2}$ and $\xi = R\hbar\omega_\perp/2\mu$ are the Thomas-Fermi radius and the healing length respectively.

In the general case of an interacting gas at finite temperature, we have to evaluate numerically the total energy as the sum of four terms [38],

$$E_\kappa = E_{\text{kin,c}} + E_{\text{trap}} + E_{\text{int}} + E_{\text{kin,T}}. \quad (3.5)$$

These terms are the kinetic energy of the condensate

$$E_{\text{kin},c} = \int d^2r \psi^*(r) \left(-\frac{\hbar^2}{2m} \nabla^2 + \frac{\hbar^2 \kappa^2}{2mr^2} \right) \psi(r), \quad (3.6)$$

the energy of confinement

$$E_{\text{trap}} = \frac{1}{2} m \omega_{\perp}^2 \int d^2r r^2 [n_c(r) + n_{nc}(r)], \quad (3.7)$$

the interaction energy

$$E_{\text{int}} = \frac{1}{2} \int d^2r [g_2 n_c^2(r) + 4g_1 n_c(r) n_{nc}(r) + 2g_1 n_{nc}^2(r)], \quad (3.8)$$

and the kinetic energy of the thermal cloud

$$E_{\text{kin},T} = \int d^2r \int \frac{dp}{2\pi\hbar^2} \frac{p^3}{2m} \{ \exp[\beta(p^2/2m + V_{\text{eff}}(r) - \mu)] - 1 \}^{-1}. \quad (3.9)$$

In Sec. (3.1.3) I compare the angular frequency obtained by the calculation of the total energy of the gas with and without a vortex with those obtained from a Thomas-Fermi calculation and from extrapolating Eq. (3.4) at finite temperature through the temperature dependence of the chemical potential.

3.1.3 Numerical result for single vortex

For a numerical illustration we have taken $\kappa = 1$ and chosen values values of particle number, the radial trap frequency, and the scattering length as appropriate for ^{23}Na atoms in the experiment of Görlitz *et al.*[17] ($N = 5 \times 10^5$, $\omega_{\perp} = 188.4 \text{ Hz}$, $a = 2.8 \text{ nm}$). I implicitly assume, however, that the trap has been axially squeezed to reach the strictly 2D scattering regime. The density profiles obtained from the solution of Eqs. (3.1) for the gas at three different values of the temperature (in units of the critical temperature $T_c = (\sqrt{6N}/\pi k_B) \hbar \omega_{\perp}$ of the ideal Bose gas) are shown in Figs. 3.1 and 3.2. In the absence of a vortex (Fig. 3.1), the main point to notice is that the growth of the thermal cloud exerts an increasing repulsion on the outer parts of the condensate, constricting it towards the central region of the trap.

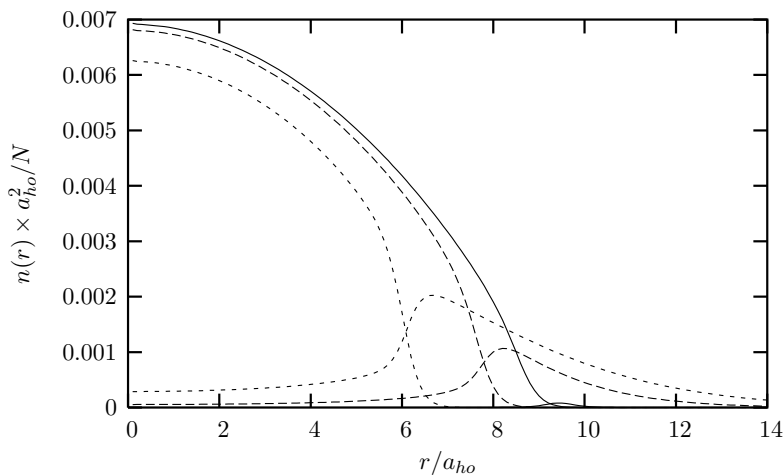


Figure 3.1: Density profiles $n(r)$ for the condensate and the thermal cloud (in units of a_{ho}^2/N , with $a_{ho} = \sqrt{\hbar/m\omega_{\perp}}$) versus radial distance r (in units of a_{ho}) at temperature $T/T_c = 0.05$ (full line), 0.25 (long-dashed line), and 0.50 (short-dashed line).

This effect is seen only when the condensate is treated by the NLSE and persists in the presence of a vortex (Fig. 3.2), but as we shall see below, is missed in the Thomas-Fermi approximation where the radial kinetic energy of the condensate is neglected. In addition, the thermal cloud penetrates the core of the vortex and enhances the expulsion of the condensate from the core region (inset of Fig. 3.2), in a manner which again is governed in its details by the radial kinetic energy term in the NLSE. The profiles obtained for a BEC containing a vortex at $T = 0.5 T_c$ by the full numerical calculation using the NLSE are compared in Fig. 3.3 with those obtained in the Thomas-Fermi approximation. The constriction of the condensate in its outer parts and its expulsion from the core region by the thermal cloud are clearly underestimated in the Thomas-Fermi theory. Finally, Fig. 3.4 reports our results for the energy of the vortex as a function of T/T_c . The inaccuracies arising in the density profiles from the Thomas-Fermi treatment of the interplay between the condensate and the thermal cloud clearly lead to large errors in the estimation of $\Omega_c(T)$. On the other hand the simple expression given in Eq. (3.4), with the two alternatives of using in it the

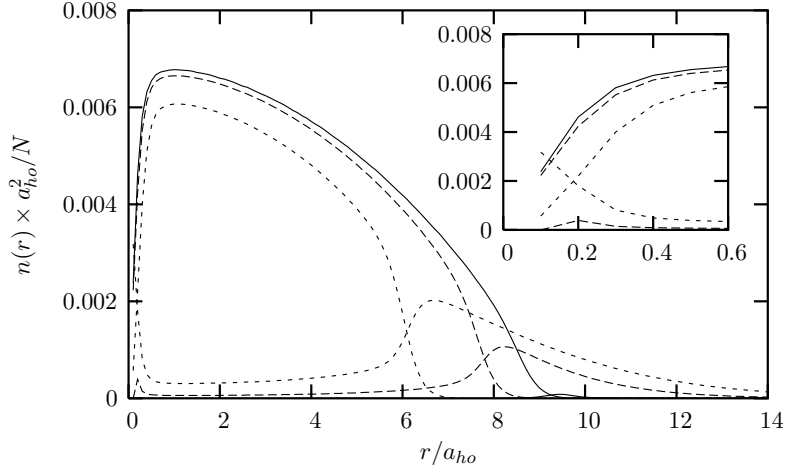


Figure 3.2: Density profiles for the condensate and for the thermal cloud in the presence of a vortex. Units and symbols are as in Fig. 3.1. The inset shows an enlarged view of the profiles near the center of the trap.

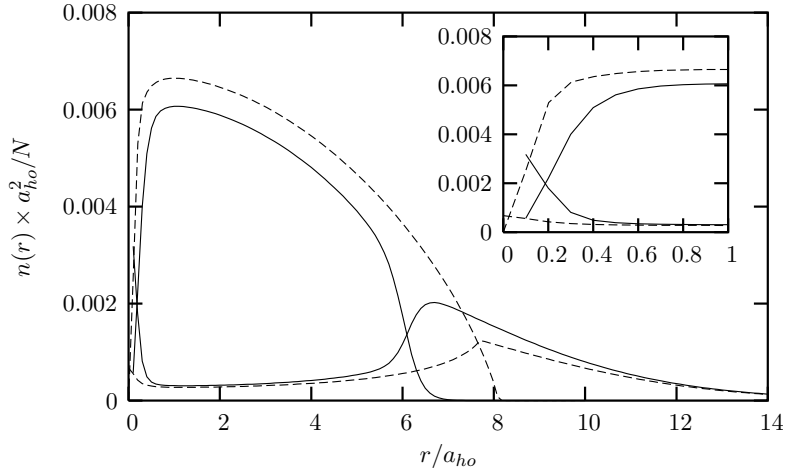


Figure 3.3: Density profiles for a BEC containing a vortex at $T/T_c = 0.50$ in the full calculation using the NLSE (full lines) and in the Thomas-Fermi approximation (dashed lines). The units are as in Fig. 3.1. The inset shows an enlarged view of the profiles near the center of the trap.

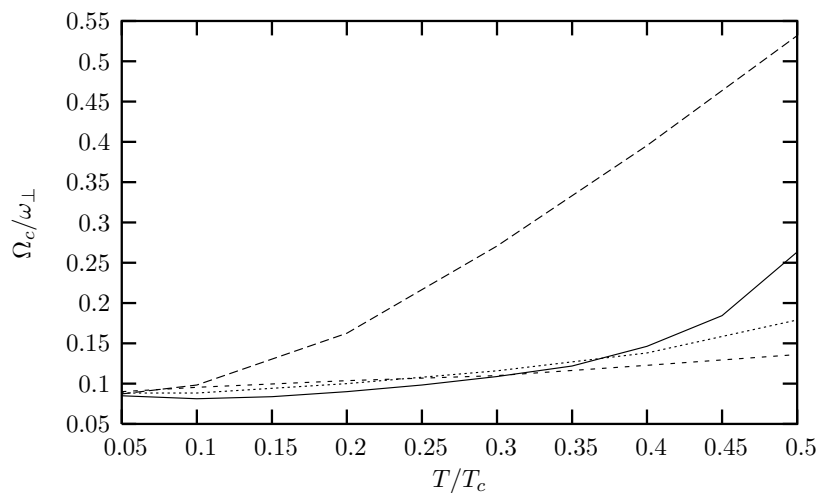


Figure 3.4: The energy of a vortex, expressed as the thermodynamic critical frequency Ω_c in units of the radial trap frequency ω_{\perp} , as a function of T/T_c . The results from the full calculation using the NLSE (full line) are compared with those obtained from Eq. (3.4) with the corresponding values of $\mu(T)$ (dotted line) and with the Thomas-Fermi values of $\mu(T)$ (short-dashed line). The long-dashed line shows the results obtained in a calculation using the Thomas-Fermi theory.

chemical potential $\mu(T)$ from the Thomas-Fermi approximation or from the full calculation using the NLSE, gives a reasonable account of the vortex energy up to $T \simeq 0.5 T_c$.

3.2 Density Functional Theory for many-vortex problem

3.2.1 Introduction

Nelson et al. [73] have shown that the statistical mechanics of the flux-line lattice (FLL) of high- T_c superconductors can be studied through an appropriate mapping onto the 2D Yukawa boson system interacting with potential $V_Y(r) = \epsilon K_0(r/\sigma)$ where ϵ is an energy scale and σ is a length scale having the meaning of a screening length. The function $K_0(x)$ being the modified Bessel function and the coefficient ϵ attached to it is the coupling strength that scales the energy of interaction.

The Hamiltonian of N bosons describing this system reads

$$H = - \sum_i \Lambda^2 \nabla_i^2 + \sum_{i < j} K_0(r_{ij}). \quad (3.10)$$

Here i, j are particle indices and the de Boer dimensionless parameter is defined by $\Lambda^2 = \hbar^2/2m\sigma^2\epsilon$. Meanwhile the reduced density of the system is denoted by $\rho = N/A\sigma^2$, where A is the surface area. These two dimensionless parameter characterize the system.

On the other hand, the Hamiltonian for a system of N vortices mapped as a system of N boson interacting with Yukawa potential is written as

$$H = - \sum_i \frac{(k_B T)^2}{2\tilde{\epsilon}} \nabla_i^2 + \sum_{i < j} \frac{\phi_0^2}{8\pi^2 \lambda^2} K_0(r_{ij}/\lambda). \quad (3.11)$$

The system described by the Hamiltonian (3.11) is equal to one described by Hamiltonian (3.10) if we set $\sigma = \lambda$ and $\Lambda^2 = (2\pi k_B T)^2/2\tilde{\epsilon}\phi_0^2$.

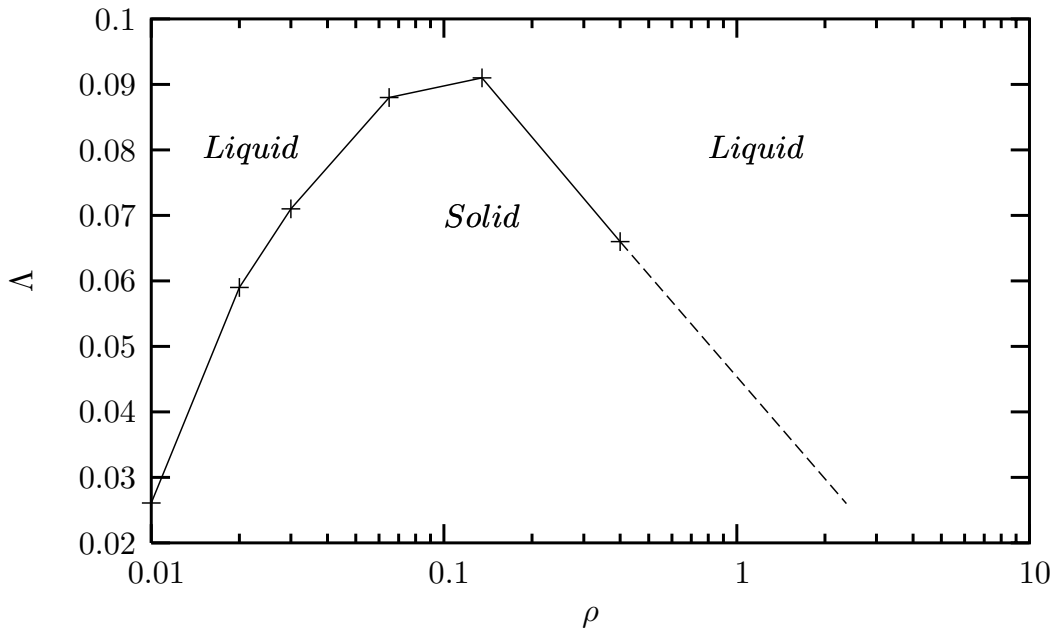


Figure 3.5: The phase diagram of Yukawa bosons reproduced from Magro and Ceperley [74]. The pluses are transition points computed with DMC. The dashed lines at high densities is the scaling law: $\Lambda \sim 0.04/\sqrt{\rho}$.

Following this idea, Magro and Ceperley [74, 75] have performed a Diffusion Monte Carlo (DMC) and Variational Monte Carlo (VMC) numerical calculation to calibrate the ground state vortex properties for a homogeneous 2D Yukawa boson system. Of particular interest to us is the phase diagram obtained for the data of (ρ, Λ) at transition points displayed in Fig (3.5).

They observed that for a particular region $\Lambda > 0.09$ the system is dominated by kinetic energy and does not crystallize. Below this threshold however a peculiar behaviour of reentrant liquid has been observed. Which means that system is in the liquid phase at very low density as well at high density. The crystal melts on compression and expansion. Nevertheless this reentrant liquid behaviour has not been fully understood.

Inspired by their work, I will investigate the ground state property of a system of N vortices mapped as N bosons interacting *via* 2D Yukawa potential $V(x) = \epsilon K_0(x)$ confined in a 2D harmonic planar geometry $\frac{1}{2}m\omega_{\perp}^2 \mathbf{r}^2$. As a

matter of fact, the Yukawa potential has an interesting combination of short range with soft core. For small x , $K_0(x)$ diverges like $-\ln(x)$ while for large x it decays as $\exp(-x)/\sqrt{x}$. The logarithmic term represents the inter-vortex repulsion and the exponential decay signifies that vortices far apart do not feel each other.

3.2.2 Density Functional Theory

With the Yukawa potential we cannot use the similar approach used for the contact delta potential $V_0\delta(\mathbf{r}-\mathbf{r}')$ in deriving a dynamical equation of motion as described in chapter 1. Here we use the Density functional theory (DFT) which is originally based on the notion that for a many-electron system there is a one-to-one mapping between the external potential and the electron density: $v_{ext}(\mathbf{r}) \leftrightarrow \rho(\mathbf{r})$. In other words, the density is uniquely determined given a potential, and *vice versa*. All properties are therefore a functional of the density, because the density determines the potential, which determines the Hamiltonian, which determines the energy and the wave function .

Following this train of reasoning, the inhomogeneous dilute system of N interacting bosons can be described within the second quantization language as

$$\begin{aligned}\hat{H} &= \hat{H}_0 + \int d\mathbf{r} \psi^\dagger(\mathbf{r}) V_{ext}(\mathbf{r}) \psi(\mathbf{r}) \\ &+ \frac{1}{2} \int d\mathbf{r} \int d\mathbf{r}' \psi^\dagger(\mathbf{r}) \psi^\dagger(\mathbf{r}') V(|\mathbf{r}-\mathbf{r}'|) \psi(\mathbf{r}') \psi(\mathbf{r}) \\ &= \hat{H}_0 + \hat{V}_{ext} + \hat{V}_{int}\end{aligned}\tag{3.12}$$

where $\hat{H}_0 = \int d\mathbf{r} \psi^\dagger(\mathbf{r}) \left[-\frac{\hbar^2}{2m} \nabla^2 - \mu \right] \psi(\mathbf{r})$ and $V(|\mathbf{r}-\mathbf{r}'|)$ is the inter-atomic interaction potential. The annihilation and creation field operators are denoted by $\psi^\dagger(\mathbf{r})$ and $\psi(\mathbf{r}')$ respectively and obey Bose-Einstein commutation relations:

$$[\psi(\mathbf{r}), \psi^\dagger(\mathbf{r}')] = \delta(\mathbf{r}-\mathbf{r}') \quad [\psi(\mathbf{r}), \psi(\mathbf{r}')] = [\psi^\dagger(\mathbf{r}), \psi^\dagger(\mathbf{r}')] = 0.\tag{3.13}$$

Let us denote the ground state of the system as $|g\rangle$ so the ground state energy is defined as $E_0 = \langle g | \hat{H} | g \rangle$ and the density as $n(\mathbf{r}) = \langle g | \psi^\dagger \psi | g \rangle$. The Hohenberg-Kohn (HK) theorem [113] guarantees that there exists a unique functional of the density,

$$F[n(\mathbf{r})] = \langle g | \hat{H}_0 + \hat{V}_{int} | g \rangle , \quad (3.14)$$

irrespective of the external potential. The theorem was originally proved for fermions but its generalization also covers bosons. Following HK, we can write the total energy functional of the system as following,

$$E[n(\mathbf{r})] = F[n(\mathbf{r})] + \int d\mathbf{r} V_{ext}(\mathbf{r}) n(\mathbf{r}) \quad (3.15)$$

Determination of the ground state energy follows by imposing the stationary conditions

$$\frac{\delta E[n(\mathbf{r})]}{\delta n(\mathbf{r})} = 0 \quad (3.16)$$

In general, the ground state cannot be determined exactly, but one has to resort to the Kohn-Sham procedure [114] to introduce an accurate approximation. The idea is to map the interacting system of interest to an auxiliary system. In order to describe the auxiliary system, let us first decompose the Bose quantum field operators $\psi(\mathbf{r})$ as a sum of spatially varying condensate $\Phi(\mathbf{r})$ and a fluctuation field operator $\tilde{\psi}$:

$$\psi(\mathbf{r}) = \Phi(\mathbf{r}) + \tilde{\psi}(\mathbf{r}) \quad , \quad \psi^\dagger(\mathbf{r}) = \Phi^*(\mathbf{r}) + \tilde{\psi}^\dagger(\mathbf{r}) \quad (3.17)$$

The wave function $\Phi(\mathbf{r})$ is also known as the order parameter and is defined as the statistical average of the particle field operator $\Phi(\mathbf{r}) = \langle \psi \rangle$. On the other hand, the condensate density is defined in term of order parameter as $n_c(\mathbf{r}) = |\Phi(\mathbf{r})|^2$. In the well-known Bogoliubov approximation [24] for a dilute weakly interacting gas, in which almost all the atoms are Bose condensed, one keeps only the term up to quadratic in the non-condensate field operators $\tilde{\psi}$ and $\tilde{\psi}^\dagger$. When the fluctuation field is comparably small to the spatial order parameter (in an average sense, $\tilde{\psi} \ll \Phi$) one can comfortably utilise a Mean-field approach. Using the decomposition in Eq.(3.17) above and

applying the Bogoliubov approximation, one can replace the product of field operators $\psi^\dagger(\mathbf{r})\psi^\dagger(\mathbf{r}')\psi(\mathbf{r}')\psi(\mathbf{r})$ in the interaction energy term of Eq.(3.12) by

$$\begin{aligned} \psi^\dagger(\mathbf{r})\psi^\dagger(\mathbf{r}')\psi(\mathbf{r}')\psi(\mathbf{r}) &= |\Phi(\mathbf{r})|^2|\Phi(\mathbf{r}')|^2 + 2|\Phi(\mathbf{r})|^2 \left[\Phi(\mathbf{r}')\tilde{\psi}^\dagger(\mathbf{r}') + \Phi^*(\mathbf{r}')\tilde{\psi}(\mathbf{r}') \right] \\ &+ |\Phi(\mathbf{r}')|^2\tilde{\psi}^\dagger(\mathbf{r})\tilde{\psi}(\mathbf{r}) + \Phi^*(\mathbf{r}')\Phi(\mathbf{r})\tilde{\psi}^\dagger(\mathbf{r})\tilde{\psi}(\mathbf{r}') \\ &+ \frac{1}{2}\Phi^*(\mathbf{r}')\Phi^*(\mathbf{r})\tilde{\psi}(\mathbf{r})\tilde{\psi}(\mathbf{r}') + \frac{1}{2}\Phi(\mathbf{r}')\Phi(\mathbf{r})\tilde{\psi}^\dagger(\mathbf{r})\tilde{\psi}^\dagger(\mathbf{r}') \end{aligned} \quad (3.18)$$

So now we are in a position to define the Hamiltonian of the auxiliary system that includes the inter-particle potential defined above as

$$\hat{H}^s = \int d\mathbf{r} \psi^\dagger(\mathbf{r}) \left[-\frac{\hbar^2}{2m} \nabla^2 - \mu \right] \psi(\mathbf{r}) + \hat{V}_s + \int d\mathbf{r} \psi^\dagger(\mathbf{r}) V_{ext}^s(\mathbf{r}) \psi(\mathbf{r}). \quad (3.19)$$

where our definition of auxiliary interparticle potential reads

$$\begin{aligned} \hat{V}_s &= \int d\mathbf{r} \int d\mathbf{r}' V(|\mathbf{r} - \mathbf{r}'|) |\Phi(\mathbf{r})|^2 \left[\Phi(\mathbf{r}')\tilde{\psi}^\dagger(\mathbf{r}') + \Phi^*(\mathbf{r}')\tilde{\psi}(\mathbf{r}') \right] \\ &+ \frac{1}{2} \int d\mathbf{r} \int d\mathbf{r}' V(|\mathbf{r} - \mathbf{r}'|) [2\Phi^*(\mathbf{r}')\Phi(\mathbf{r})\tilde{\psi}^\dagger(\mathbf{r})\tilde{\psi}(\mathbf{r}') \\ &+ \Phi(\mathbf{r}')\Phi(\mathbf{r})\tilde{\psi}^\dagger(\mathbf{r})\tilde{\psi}^\dagger(\mathbf{r}') + \Phi^*(\mathbf{r}')\Phi^*(\mathbf{r})\tilde{\psi}(\mathbf{r})\tilde{\psi}(\mathbf{r}')]. \end{aligned} \quad (3.20)$$

Thus for the ground state $|g_s\rangle$ we can define the unique ground state energy functional of the auxiliary system as

$$F^s[n_s(\mathbf{r})] = \langle g_s | \int d\mathbf{r} \psi^\dagger(\mathbf{r}) \left[-\frac{\hbar^2}{2m} \nabla^2 - \mu \right] \psi(\mathbf{r}) |g_s\rangle + \langle g_s | \hat{V}_s |g_s\rangle, \quad (3.21)$$

which does not depend on the auxiliary external potential V_{ext}^s . Hence, the total energy functional of the auxiliary system can be written as

$$E^s[n_s(\mathbf{r})] = F^s[n_s(\mathbf{r})] + \int d\mathbf{r} n(\mathbf{r}) V_{ext}^s(\mathbf{r}) \quad (3.22)$$

in which $E^s[n_s(\mathbf{r})]$ can be approximated to $E[n(\mathbf{r})]$ or in other word the density of the auxiliary system $n_s(\mathbf{r})$ is identical to the real system $n(\mathbf{r})$ by choosing a proper choice of auxiliary external potential V_{ext}^s .

Since the non-interacting part of Eq. (3.21) is equal to the non-interacting part of Eq. (3.14) and comparing terms in Eq.(3.20) with Eq. (3.18) we obtain the following functional relation:

$$F[n(\mathbf{r})] = F^s[n(\mathbf{r})] + \int d\mathbf{r} \int d\mathbf{r}' V(\mathbf{r} - \mathbf{r}') n(\mathbf{r}) n(\mathbf{r}') + F_{xc}[n(\mathbf{r})]. \quad (3.23)$$

The second term \hat{V}_H is called the Hartree-energy defined as

$$\hat{V}_H = \frac{1}{2} \int d\mathbf{r} \int d\mathbf{r}' V(|\mathbf{r} - \mathbf{r}'|) n(\mathbf{r}) n(\mathbf{r}') \quad (3.24)$$

in which the total density $n(\mathbf{r})$ includes a non-condensate local density defined as

$$\tilde{n}(\mathbf{r}) \equiv \langle \tilde{\psi}^\dagger(\mathbf{r}) \tilde{\psi}(\mathbf{r}) \rangle = n(\mathbf{r}) - |\Phi(\mathbf{r})|^2. \quad (3.25)$$

The last term in Eq. (3.23) represents the exchange-correlation energy $E_{xc}[n(\mathbf{r})]$ and includes all the contributions to the interaction energy beyond mean field. Calculating the variational derivatives in Eq. (3.16) using Eq.(3.23), one finds

$$\frac{\delta F^s[n(\mathbf{r})]}{\delta n(\mathbf{r})} + V_H(\mathbf{r}) + \frac{\delta F_{xc}[n(\mathbf{r})]}{\delta n(\mathbf{r})} + V_{ext}(\mathbf{r}) = 0 \quad (3.26)$$

where the Hartree field read

$$V_H(\mathbf{r}) = \int d\mathbf{r}' V(|\mathbf{r} - \mathbf{r}'|) n(\mathbf{r}'). \quad (3.27)$$

Performing a similar variational calculation on Eq. (3.22) we deduce that the density of the auxiliary system is identical to the actual system if

$$V_{ext}^s(\mathbf{r}) = V_{ext}(\mathbf{r}) + V_H(\mathbf{r}) + \frac{\delta F_{xc}[n(\mathbf{r})]}{\delta n(\mathbf{r})}. \quad (3.28)$$

3.2.3 Interacting auxiliary system : Bogoliubov approach

In general, if an interacting auxiliary system is chosen, one needs to do further analysis by using a Bogoliubov approach. We rewrite the auxiliary Hamiltonian Eq. (3.19) using the decomposition in Eq. (3.17) by

$$\begin{aligned} \hat{H}^s &= \int d\mathbf{r} \Phi^*(\mathbf{r}) L \Phi(\mathbf{r}) + \int d\mathbf{r} \tilde{\psi}^\dagger(\mathbf{r}) L \Phi(\mathbf{r}) + \int d\mathbf{r} \Phi^*(\mathbf{r}) L \tilde{\psi}(\mathbf{r}) \\ &+ \int d\mathbf{r} \tilde{\psi}^\dagger(\mathbf{r}) L \tilde{\psi}(\mathbf{r}) + \frac{1}{2} \int d\mathbf{r} \int d\mathbf{r}' V_Y(|\mathbf{r} - \mathbf{r}'|) [2\Phi^*(\mathbf{r}') \Phi(\mathbf{r}) \tilde{\psi}^\dagger(\mathbf{r}) \tilde{\psi}(\mathbf{r}')] \\ &+ \Phi(\mathbf{r}') \Phi(\mathbf{r}) \tilde{\psi}^\dagger(\mathbf{r}) \tilde{\psi}^\dagger(\mathbf{r}') + \Phi^*(\mathbf{r}') \Phi^*(\mathbf{r}) \tilde{\psi}(\mathbf{r}) \tilde{\psi}(\mathbf{r}')] \end{aligned} \quad (3.29)$$

where the operator \hat{L} is defined by

$$\hat{L} \equiv \left(-\frac{\nabla^2}{2m} + V_{ext}^s - \mu \right). \quad (3.30)$$

In order to diagonalize Eq. (3.29), we first eliminate the terms linear in $\tilde{\psi}$ and $\tilde{\psi}^\dagger$ by requiring that $\Phi(\mathbf{r})$ satisfy the equation

$$\hat{L}\Phi(\mathbf{r}) = 0. \quad (3.31)$$

Hence our auxiliary Hamiltonian Eq. (3.29) reduces to

$$\begin{aligned} \hat{H}^s &= \int d\mathbf{r} \tilde{\psi}^\dagger(\mathbf{r}) L \tilde{\psi}(\mathbf{r}) + \int d\mathbf{r} \int d\mathbf{r}' V(|\mathbf{r} - \mathbf{r}'|) \Phi^*(\mathbf{r}') \Phi(\mathbf{r}) \tilde{\psi}^\dagger(\mathbf{r}) \tilde{\psi}(\mathbf{r}') \\ &+ \frac{1}{2} \int d\mathbf{r} \int d\mathbf{r}' V(|\mathbf{r} - \mathbf{r}'|) [\Phi(\mathbf{r}') \Phi(\mathbf{r}) \tilde{\psi}^\dagger(\mathbf{r}) \tilde{\psi}^\dagger(\mathbf{r}') \\ &+ \Phi^*(\mathbf{r}') \Phi^*(\mathbf{r}) \tilde{\psi}(\mathbf{r}) \tilde{\psi}(\mathbf{r}')]. \end{aligned} \quad (3.32)$$

The quadratic expression given by this equation can be diagonalized by the usual Bogoliubov transformation [24]

$$\begin{aligned} \tilde{\psi}(\mathbf{r}) &= \sum_i [u_i(\mathbf{r}) \alpha_i - v_i^*(\mathbf{r}) \alpha_i^\dagger] \\ \tilde{\psi}^\dagger(\mathbf{r}) &= \sum_i [u_i^*(\mathbf{r}) \alpha_i^\dagger - v_i(\mathbf{r}) \alpha_i], \end{aligned} \quad (3.33)$$

where the quasiparticle operators α_i and α_i^\dagger satisfy Bose commutation relations. The values of u_i and v_i are obtained by solving the following coupled Bogoliubov equations:

$$\begin{aligned} \hat{L}u_i &+ \int d\mathbf{r}' V(|\mathbf{r} - \mathbf{r}'|) \Phi^*(\mathbf{r}') \Phi(\mathbf{r}) u_i(\mathbf{r}') \\ &+ \int d\mathbf{r}' V(|\mathbf{r} - \mathbf{r}'|) \Phi(\mathbf{r}') \Phi(\mathbf{r}) v_i(\mathbf{r}') = E_i u_i(\mathbf{r}) \end{aligned} \quad (3.34)$$

and

$$\begin{aligned} \hat{L}v_i &+ \int d\mathbf{r}' V(|\mathbf{r} - \mathbf{r}'|) \Phi^*(\mathbf{r}) \Phi(\mathbf{r}') v_i(\mathbf{r}') \\ &+ \int d\mathbf{r}' V(|\mathbf{r} - \mathbf{r}'|) \Phi^*(\mathbf{r}) \Phi^*(\mathbf{r}') u_i(\mathbf{r}') = -E_i v_i(\mathbf{r}). \end{aligned} \quad (3.35)$$

Hence with the solution of u_i and v_i from the above coupled equations, the Hamiltonian in Eq. (3.29) can be shown to reduce to

$$\hat{H}_{new}^s = - \sum_i E_i \int d\mathbf{r} |v_j(\mathbf{r})|^2 + \sum_i E_i \alpha_i^\dagger \alpha_i, \quad (3.36)$$

which describes a non-interacting gas of quasiparticles of energy E_j . The ground state expectation value of Eq. (3.36) is given by

$$E_0^s = - \sum_i E_i \int d\mathbf{r} |v_j(\mathbf{r})|^2, \quad (3.37)$$

taking into consideration that the ground state $|g_s\rangle$ obeys $\alpha |g_s\rangle = 0$. Besides, using Eq. (3.33), the local non-condensate density defined in Eq. (3.25) can be written as

$$\tilde{n}(\mathbf{r}') \equiv \langle g_s | \tilde{\psi}^\dagger(\mathbf{r}) \tilde{\psi}(\mathbf{r}) | g_s \rangle = \sum_i |v_i(\mathbf{r})|^2. \quad (3.38)$$

Thus performing a little algebra, the new auxiliary functional which includes depletion of the condensate is defined by

$$F_s[n(\mathbf{r})] = \int d\mathbf{r} \Phi^*(\mathbf{r}) \left(-\frac{\nabla^2}{2m} - \mu \right) \Phi(\mathbf{r}) - \sum_i \int d\mathbf{r} |v_i(\mathbf{r})|^2 [E_j + V_s(\mathbf{r})]. \quad (3.39)$$

The key element in the above derivation is that one can take into account the depletion of the condensate as shown in Eq. (3.38). Using the the auxiliary system defined by the Hamiltonian Eq. (3.19) and the relation in Eq (3.28), both the condensate density $n_c \equiv |\Phi(\mathbf{r})|^2$ and also the total density $n(\mathbf{r})$ can be computed.

The difficulties in finding the solution for Eq. (3.31), Eqs (3.34) and (3.35) lies in the fact that the exact functional dependence of the exchange-correlation potential $v_{xc}[n(\mathbf{r})] = \delta F_{xc}[n(\mathbf{r})]/\delta n(\mathbf{r})$ is unknown for most of the system of interest and thus one has to resort to approximations such as the Local Density Approximation (LDA).

3.2.4 Application of DFT to N vortex problem

We are now in a position to analyse our problem of N vortices treated as N Yukawa bosons via the one-to-one mapping of Nelson and Seung [73] with the DFT tool summarized in the previous section within our appropriate scaling. By choosing an auxiliary system of N non-interacting bosons (referring to Eq. (3.21) and Eq. (3.28)), Eq. (3.31) then can be written more explicitly as satisfying the following equation:

$$\left(-\frac{\hbar^2}{2m}\nabla^2 + V_{ext}(\mathbf{r}) + V_H(\mathbf{r}) + \frac{\delta F_{xc}[n(\mathbf{r})]}{\delta n(\mathbf{r})} \right) \Phi(\mathbf{r}) = \mu\Phi(\mathbf{r}). \quad (3.40)$$

This equation is a sort of generalization of Gross-Pitaevskii equation for a dilute inhomogeneous gas at $T = 0$. Since we have chosen a non-interacting auxiliary system, we expect that at $T = 0$ all the atoms are Bose condensed as their total density $n(\mathbf{r})$ is approximated by condensate density $n_c(\mathbf{r}) = |\Phi(\mathbf{r})|^2$. Setting $F_{xc}[n(\mathbf{r})] = 0$ one recovers a closed non-linear Schrödinger equation (NLSE).

The available numerical data of Magro and Ceperley [74] and Strepparola et. al [115] permit one to obtain information on the homogeneous excess free energy $f_{ex}[n]$ rather than the homogeneous exchange correlation energy $f_{xc}[n]$. Thus it is much convenient to work with excess free energy defined as [116]

$$F_{ex}[n(\mathbf{r})] = \hat{V}_H[n(\mathbf{r})] + F_{xc}[n(\mathbf{r})]. \quad (3.41)$$

In general, the excess correlation functional energy $F_{ex}[n(\mathbf{r})]$ in a DFT calculation is not known exactly. One can resort to approximations such as the Local density approximation (LDA) which reads,

$$F_{ex}[n(\mathbf{r})] \approx \int d\mathbf{r} F_{ex}^{hom}[n]|_{n \rightarrow n(\mathbf{r})} \quad (3.42)$$

where $F_{ex}^{hom}[n] = n f_{ex}^{hom}[n]$. The functional derivatives (excess-correlation potential) of the above relation can be written as [117, 118]

$$V_{ex}(\mathbf{r}, n(\mathbf{r})) = \frac{\delta F_{ex}[n(\mathbf{r})]}{\delta n(\mathbf{r})} = \frac{\partial(n f_{ex}[n])}{\partial n}|_{n \rightarrow n(\mathbf{r})}. \quad (3.43)$$

Information of the homogeneous excess correlation energy $f_{ex}[n]$ can be obtained by subtracting the kinetic energy from the total ground state energy of a homogeneous system with N boson. A plot of the DMC data of Magro and Ceperley [74] and the STLS data of Strepparola et. al. [115] are depicted along with the following fit

$$f_{ex}[\rho] = \frac{2\rho}{\ln(1/\rho)}, \quad (3.44)$$

in Fig (3.6). To be consistent with the scaling of Magro and Ceperley [74] I will scale all lengths by harmonic oscillator length $\sigma = \sqrt{\hbar/m\omega_{\perp}}$ and the energy by $\epsilon = \hbar\omega_{\perp}/2$. Eq. (3.40) is solved numerically using the excess correlation potentials of Eq.(3.43) and Eq. (3.44) self-consistently with the condition that the areal integral of the condensate density $|\Phi(\mathbf{r})|^2$ is equal to the total number N of bosons.

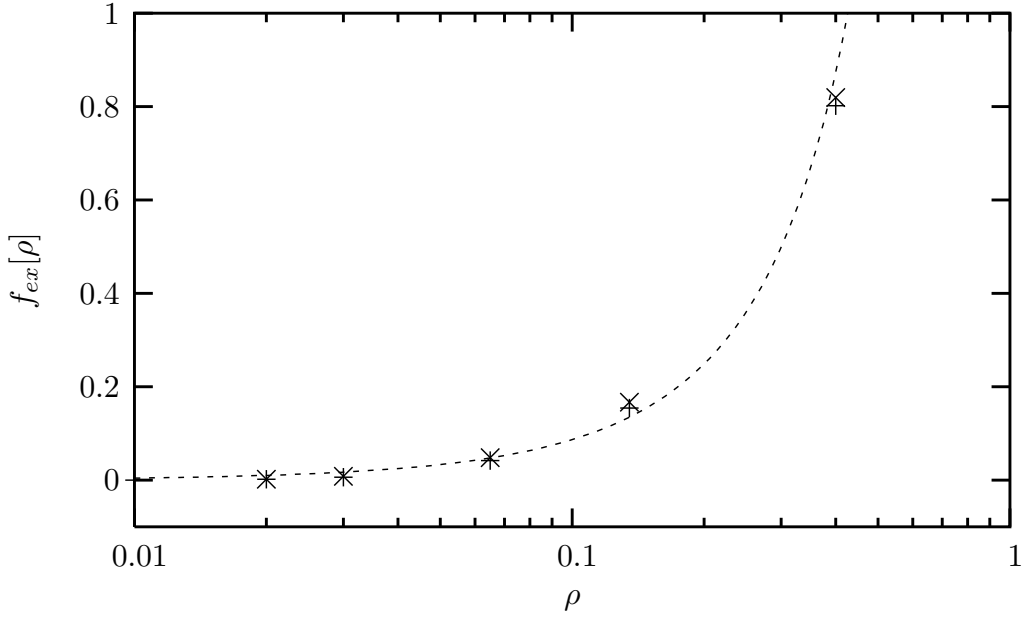


Figure 3.6: Homogeneous excess-correlation energy $f_{ex}(\rho)$ versus the dimensionless homogeneous density ρ gas of the VMC data of Magro and Ceperley [74] (pluses) and STLS data of Strepparola et. al. [115] (crosses) compared to the fit function Eq. (3.44) (dashed-lines).

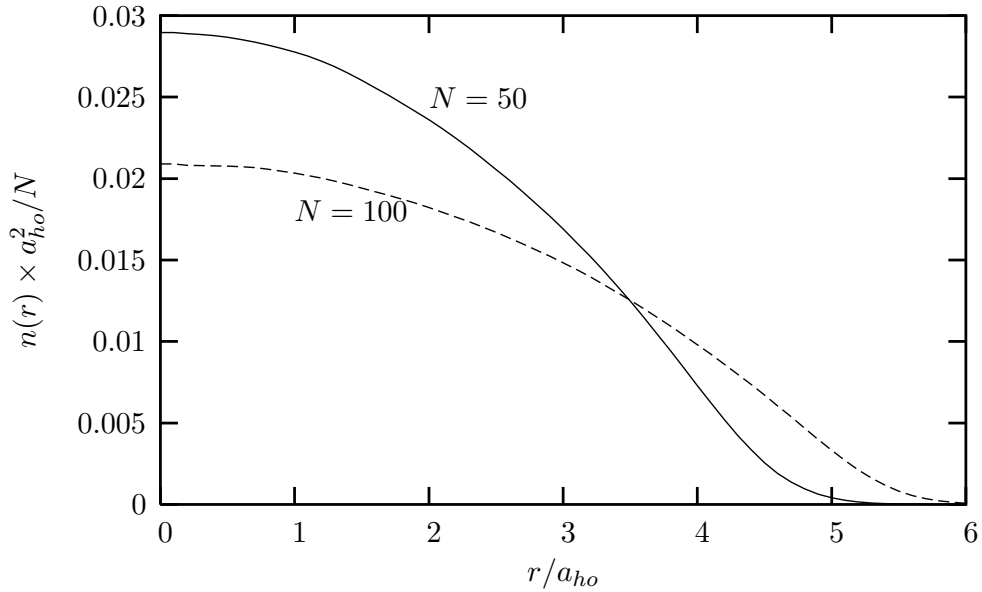


Figure 3.7: Density profiles $n(r)$ for the condensate (in units a_{ho}^2/N , with $a_{ho} = \sqrt{\hbar/m\omega_{\perp}}$) versus the radial distance r (in units a_{ho}) obtained using Eq.(3.40) for $N = 50$ and $N = 100$ bosons

Chapter 4

Summary and Future Direction

4.1 Summary and future directions

In this thesis I have reported on the development on some fundamental microscopic aspects of a two-dimensional Bose-Einstein condensate at finite temperature. The approach presented here is of mean-field nature which obeys the spontaneous symmetry breaking. This leads to a nonzero mean value of the atomic Bose field operator, which corresponds to the order parameter for the BEC phase transition. The order parameter which describes the mean-field condensate is highly correlated with quantum fluctuations. The condensate which is well described by the Gross-Pitaevskii equation is coupled with the Hartree-Fock model of the thermal cloud. We call this the two-fluid model description in this thesis.

Phase fluctuations and scattering properties play a crucial role in the studies of 2D Bose gas. One important consequence of lowered dimensionality is that the T-matrix for two-body collisions *in vacuo* at low momenta and energy, which should be used to obtain the collisional coupling parameter to the lowest order in the particle density, vanishes in the strictly 2D limit as the *s*-wave scattering length becomes larger than the width of the axial trapping [40, 12]. It is then necessary to evaluate the scattering processes between pairs of Bose particles in by taking into account the presence of a

condensate and a thermal cloud through a many-body T-matrix formalism [82, 83, 84]. In fact in this thesis I have calculated the many-body T-matrix which includes the effect of thermal excitations. I have found that the many-body screening of the interactions due to the occupancy of excited states is quite large and rapidly increasing with temperature. However such many-body screening has, however, very little effect on equilibrium properties of the gas for our choice of system parameters for the temperature of interest in this work ($T \leq 0.5 T_c$). This work has been published as “Density profile of a strictly two-dimensional Bose gas at finite temperature”, K. K. Rajagopal, P. Vignolo and M. P. Tosi, *Physica B* **344**,157 (2004).

Measurement of Feshbach resonances provides a means of obtaining information about interaction strength (repulsive $g > 0$ or attractive $g < 0$) between atoms. The exact location and width are very important in deducing the interatomic potentials, but to our knowledge they have not been calculated or measured experimentally for the strictly 2D case. Series of calculation for different species of atomic gasses for the 3D cases can be found in the literature [39, 94, 119, 93, 103].

In this thesis I have explicitly applied the formalism already developed to treat Feshbach resonances in 3D boson gases to the case of a 2D Bose gas at zero temperature. One of the main results is that an external magnetic field could be used to drive the coupling from repulsive to attractive even in a pancake geometry as the scattering length becomes larger than the axial width of the condensed cloud. For the case of repulsive interactions I have evaluated the particle density profiles at varying coupling strength, demonstrating the approach to a Thomas-Fermi profile followed by collapse. In the opposite regime of attractive coupling I have given an estimate for the critical number of bosons that can form a stable condensate. I found that this critical number is inversely proportional to the absolute magnitude of the coupling, independently of the strength of the in-plane confinement. This work has been published as “Feshbach resonances in a strictly two-dimensional atomic Bose gas”, K. K. Rajagopal, P. Vignolo and M. P. Tosi, *Physica B* **353**, 59

(2004).

Also in this thesis I have calculated the particle density, ground state energy and critical frequency that required to nucleate a single stable vortex when a 2D condensate put into rotation at various temperatures. My calculations illustrate the interplay between the thermal cloud and the structure of the condensate in the regions where the radial kinetic energy of the condensate is playing an important role (namely, in the outer parts of the condensate and in the vortex core) and validated the use of a simple expression of the vortex energy for temperatures up to about $0.5 T_c$. This work has been published as “ Temperature dependence of the energy of a vortex in a two-dimensional Bose gas ”, K. K. Rajagopal, P. Vignolo and M. P. Tosi, *Physics Letter A* **328**, 500 (2004).

The work presented in thesis has given a broad microscopic description of homogeneous or trapped 2D Bose gas. Thus it opens up an interesting range of further research possibilities. At the same time, the generality of the approach considered here leaves numerous questions unanswered. One of them which interest me the most is the dynamics of many vortices in a 2D harmonically trapped Bose gas. In Sec. 3.2 I have developed a density functional theory (DFT) technique to calibrate the ground state properties of the vortex fluid confined in a two-dimensional harmonic trap within the Bogoliubov-de Gennes reference system.

When a non-interacting auxiliary system is inferred in the DFT model, we obtained a Kohn-Sham (KS) type equation. I have calculated numerically the density profile and the ground state energy of the vortex fluid using KS equation for $N \leq 137$ bosons. The excess-correlation potential in this equation is obtained from a fit to the liquid phase VMC data of Magro and Ceperley [74] and Strepparola et.al [115] for the homogeneous ground state energies.

The crystallization of Yukawa bosons (vortices) can be studied by making an analogy to Wigner crystallization [120] in a system of electrons. Wigner

first predicted that a system of electrons in a uniform potential would crystallize at low density within the Hartree-Fock (HF) theory. He proposed that at sufficiently low density crystallization greatly reduces the interaction energy with only a small increase in the kinetic energy. The energy lowering in the crystallization derives from the reduction of the interaction energy by spatially separating the electrons. Hartree-Fock studies have shown a transition from Fermi liquid to Wigner molecule using small number of electrons in a harmonic trap [121, 122]. This transition has been a hot topic in the last two years and often associated with the breaking of rotational symmetry found in the HF calculation of quantum dots. Very recently Romanovsky et. al.[123] have studied crystallization of bosons interacting with Coulomb potentials and contact potentials in harmonic trap for small number of particles ($N = 6$). They have demonstrated a two-step method of breaking the symmetry of strongly repelling bosons at the HF level followed by a post HF symmetry restoration incorporating a correlation beyond mean-field. The method describes transition from a BEC state to a crystalline phase in which the trap plays a crucial role in localizing the bosons. The Hartree-Fock solutions break the translational invariance of the many-body Hamiltonian and bosons are considered to be pinned as in the Wigner crystal. Their method can be used to now is to calculate the ground state properties (density profile and energy) for ($N \leq 137$) Yukawa boson in the crystalline phase.

Bibliography

- [1] A. Einstein. *Sitzungsber. Kgl. Preuss. Akad. Wiss.*, 23:3, 1925.
- [2] S. N. Bose. *Z. Phys.*, 26:178, 1924.
- [3] M. H. Anderson, J. R. Ensher, M. R. Matthews, C. E. Weimann, and E. A. Cornell. *Science*, 269:198, 1995.
- [4] K. B. Davis, M. O. Mewes, M. R. Andrews, N. J. van Druten, D. S. Durfee, D. M. Kurn, and W. Ketterle. *Phys. Rev. Lett.*, 75:3969, 1995.
- [5] C. C. Bradley, C. A. Sackett, J. J. Tollett, and R. G. Hulet. *Phys. Rev. Lett.*, 75:1687, 1995.
- [6] S. Jochim, M. Bartenstein, A. Altmeyer, G. Hendl, S. Riedl, C. Chin, J. Hecker Denschlag, and R. Grimm. *Science*, 302:2101, 2003.
- [7] M. Greiner, C. A. Regal, and D. S. Jin. *cond-matt/0311172*, 71, 2003.
- [8] C. J. Pethick and H. Smith. *Bose-Einstein Condensation in dilute Gases*. Cambridge University Press, London, 2001.
- [9] A. J. Legget. *Rev. Mod. Phys.*, 73:307, 2001.
- [10] A. S. Parkin and D. F. Walls. *Phys. Rep.*, 303:1, 1998.
- [11] A. Griffin, D. W. Snoke, and S. Stringari. *Bose-Einstein Condensation in dilute Gases*. Cambridge University Press, Cambridge, 1995.

- [12] V. N. Popov. *Functional Integral in Quantum Field Theory and Statistical Physics*. (Reidl,Dordrecht), 1983.
- [13] N. D. Mermin and H. Wagner. *Phys. Rev. Lett.*, 17:1133, 1966.
- [14] P. C. Hohenberg. *Phys. Rev.*, 158:383, 1967.
- [15] O. Penrose and L. Onsager. *Phys. Rev.*, 104:576, 1956.
- [16] J. M. Kosterlitz and D. J. Thouless. *J. Phys. C*, 6:1181, 1973.
- [17] A. Görlitz, J. M. Vogels, A. E. Leanhardt, C. Raman, T. L. Gustavson, J. R. Abo-Shaeer, A. P. Chikkatur, S. Gupta, S. Inouye, T. Rosenband, and W. Ketterle. *Phys. Rev. Lett.*, 87:130402, 2001.
- [18] A. I. Safonov, S. A. Vasilyev, I. S. Yasnikov, I. I. Lukasshevich, and S. Jaakkola. *Phys. Rev. Lett.*, 81:4545, 1998.
- [19] S. Burger, F. S. Cataliotti, C. Fort, P. Maddaloni anf F. Minardi, and M. Inguscio. *Europhys. Lett.*, 57:1, 2002.
- [20] V. Schweikhard, I. Coddington, P. Engels, V. P. Mogendorff, and E. A. Cornell. *Phys. Rev. Lett.*, 92:040404, 2004.
- [21] J. S. Langer and M. E. Fisher. *Phys. Rev. Lett.*, 19:560, 1967.
- [22] D. R. Nelson and J. M. Kosterlitz. *Phys. Rev. Lett.*, 39:1201, 1977.
- [23] D. S. Petrov, D. M. Gangardt, and G. V. Shlyapnikov. *cond-mat/0409230*, 39:1201, 1977.
- [24] N. Bogoliubov. *J. Phys. USSR*, 11:23, 1947.
- [25] K. Huang and C. N. Yang. *Phys. Rev*, 105:767, 1957.
- [26] K. Huang, C. N. Yang, and J. M. Luttinger. *Phys. Rev*, 105:776, 1957.
- [27] T. D. Lee, K. Huang, and C. N. Yang. *Phys. Rev*, 105:1119, 1957.

- [28] T. D. Lee, K. Huang, and C. N. Yang. *Phys. Rev.*, 106:1135, 1957.
- [29] E. P. Gross. *Nuovo Cimento*, 20:454, 1961.
- [30] L. P. Pitaevskii. *Zh. Eksp. Teor. Fiz.*, 40:646, 1961.
- [31] A. L. Fetter and J. D. Walecka. *Quantum Theory of Many Particle System*. McGraw-Hill, New York, 1971.
- [32] A. L. Fetter. *Phys. Rev. A.*, 53:4245, 1996.
- [33] V. V. Goldman, I.F. Silvera, and A.J. Legget. *Phys.Rev. B.*, 24:2870, 1981.
- [34] J. Oliva. *Phys.Rev. B.*, 39:4197, 1989.
- [35] T. T. Chou, C. N. Yang, and L. H. Yu. *Phys. Rev. A.*, 53:4257, 1996.
- [36] A. Minguzzi, S. Conti, and M. P. Tosi. *J. Phys.: Condens. Matter*, 9:L33, 1997.
- [37] U. Al Khawaja, J. O. Andersen, N. P. Proukakis, and H. T. C. Stoof. *Phys. Rev. A.*, 66:013615, 2002.
- [38] S. Giorgini, L. P. Pitaevskii, and S. Stringari. *J. Low Temp. Phys.*, 109:309, 1997.
- [39] A. J. Moerdijk, B. J. Verhaar, and A. Axelsson. *Phys. Rev. A.*, 51:4852, 1995.
- [40] M. Schick. *Phys. Rev. A.*, 3:1067, 1971.
- [41] Yu. Kagan, G. V. Shlyapnikov, and J. T. M. Walraven. *Phys. Rev. Lett.*, 76:2670, 1996.
- [42] H. Saito and M. Ueda. *Phys. Rev. A.*, 65:033624, 2002.
- [43] S. K. Adhikari. *Phys. Rev. A.*, 66:013611, 2002.

- [44] C. M. Savage, N. P. Robins, and J. J. Hope. *Phys. Rev. A.*, 67:014304, 2003.
- [45] D. A. Huse and E. D. Siggia. *J. Low Temp. Phys*, 46:137, 1982.
- [46] G. Baym and C. J. Pethick. *Phys. Rev. Lett.*, 76:6, 1996.
- [47] M. Ueda and A. J. Leggett. *Phys. Rev. Lett.*, 80:1576, 1998.
- [48] Y. E. Kim and A. L. Zubarev. *Phys. Lett. A*, 246:389, 1998.
- [49] A. Eleftheriou and K. Huang. *Phys. Rev. A.*, 61:043601, 200.
- [50] E. L. Andronikashvili and Y. G. Malamadze. *Rev. Mod. Phys.*, 38:567, 1966.
- [51] V. K. Tkachenko. *Zh. Eksp. Teor. Fiz.*, 49:1875, 1965.
- [52] V. K. Tkachenko. *Zh. Eksp. Teor. Fiz.*, 50:1573, 1966.
- [53] M. R. Matthews, B. P. Anderson, P. C. Haljan, D. S. Hall, C. E. Wiemann, and E. A. Cornell. *Phys. Rev. Lett.*, 83:2498, 2000.
- [54] K. W. Madison, F. Chevy, W. Wohlleben, and J. Dalibard. *Phys. Rev. Lett.*, 84:806, 2000.
- [55] K. W. Madison, F. Chevy, V. Bretin, and J. Dalibard. *Phys. Rev. Lett.*, 86:4443, 2001.
- [56] J. R. Abo-Shaeer, C. Raman, J. M. Vogels, and W. Ketterle. *Science*, 292:476, 2001.
- [57] I. Coddington, P. Engels, V. Schweikhard, and E. A. Cornell. *Phys. Rev. Lett.*, 91:100402, 2003.
- [58] T. L. Ho. *Phys. Rev. Lett.*, 87:060403, 2001.
- [59] N. K. Wilkin and J. M. F. Gunn. *Phys. Rev. Lett.*, 84:6, 2000.

- [60] N. R. Cooper, N. K. Wilkin, and J. M. F. Gunn. *Phys. Rev. Lett.*, 87:120405, 2001.
- [61] U. R. Fischer and G. Baym. *Phys. Rev. Lett.*, 90:140402, 2003.
- [62] G. Baym. *Phys. Rev. Lett.*, 91:110402, 2003.
- [63] N. K. Wilkin and J. M. F. Gunn. *Phys. Rev. Lett.*, 92:220401, 2004.
- [64] U. R. Fischer, P. O. Fedichev, and A. Recati. *J. Phys. B: At. Mol. Opt. Phys.*, 37, 2004.
- [65] J. Sinova, C. B. Hanna, and A. H. MacDonald. *Phys. Rev. Lett.*, 12:120401, 2003.
- [66] P. C. Haljan, I. Coddington, P. Engels, and E. A. Cornell. *Phys. Rev. Lett.*, 87:210403, 2001.
- [67] G. Baym. *cond-mat/0408401*, 2004.
- [68] S. Viefers, T. H. Hansson, and S. M. Riemann. *Phys. Rev. A.*, 62:053604, 2000.
- [69] A. Rozhkov and D. Stroud. *Phys.Rev. B.*, 54:R12697, 1996.
- [70] N. Regnault and Th. Jolicoeur. *Phys.Rev. B.*, 69:235309, 2004.
- [71] G. Blatter, M. V. Feigel'man, V. B. Geshkenbein, A. I. Larkin, and V. M. Vinokur. *Rev. Mod. Phys.*, 66:1125, 1994.
- [72] N. B. Kopnin. *Phys.Rev. B.*, 57:11775, 1998.
- [73] D. R. Nelson and H. S. Seung. *Phys.Rev. B.*, 39:9153, 1989.
- [74] W. R. Magro and D. M. Ceperley. *Phys.Rev. B.*, 48:411, 1993.
- [75] W. R. Magro and D. M. Ceperley. *Phys. Rev. Lett.*, 73:826, 1994.
- [76] V. Bretin, S. Stock, Y. Seurin, and J. Dalibard. *Phys. Rev. Lett.*, 92:050403, 2004.

- [77] A. A. Abrikosov. *Zh. Eksp. Teor. Fiz.*, 32:1442, 1957.
- [78] B. Tanatar, A. Minguzzi, P. Vignolo, and M. P. Tosi. *Phys. Lett. A*, 302:131, 2002.
- [79] K. K. Rajagopal, P. Vignolo, and M.P. Tosi. *Physica B*, 344:157, 2004.
- [80] O. Hosten, P. Vignolo, A. Minguzzi, B. Tanatar, and M. P. Tosi. *J. Phys. B*, 36:2455, 2003.
- [81] T. Mizushima, T. Isoshima, and K. Machida. *Phys. Rev. A.*, 64:043610, 2001.
- [82] H. T. C. Stoof and M. Bijlsma. *Phys. Rev. E*, 47:939, 1993.
- [83] M. Bijlsma and H. T. C. Stoof. *Phys. Rev. A.*, 55:498, 1997.
- [84] M. D. Lee, S. A. Morgan, M. J. Davis, and K. Burnett. *Phys. Rev. A.*, 65:043617, 2002.
- [85] U. Al Khawaja, J. O. Andersen, N. P. Proukakis, and H. T. C. Stoof. *Phys. Rev. A.*, 66:059902, 2002.
- [86] N. P. Proukakis, S. A. Morgan, S. Choi, and K. Burnett. *Phys. Rev. A.*, 58:2435, 1998.
- [87] N. P. Proukakis, K. Burnett, and H. T. C. Stoof. *Phys. Rev. A.*, 57:1230, 1998.
- [88] S. A. Morgan, M. D. Lee, and K. Burnett. *Phys. Rev. A.*, 65:022706, 2002.
- [89] P. Vignolo, A. Minguzzi, and M. P. Tosi. *Phys. Rev. A.*, 62:023604, 2000.
- [90] N. V. Prokof'ev, O. A. Ruebenacker, and B. V. Svistunov. *Phys. Rev. Lett.*, 87:270402, 2001.

- [91] F. Dalfovo, S. Giorgini, and S. Stringari. *Rev. Mod. Phys.*, 71:463, 1999.
- [92] V. Bagnato and D. Kleppner. *Phys. Rev. A.*, 44:7439, 1991.
- [93] E. Tiesinga, B. J. Verhaar, and H. T. C. Stoof. *Phys. Rev. A.*, 47:4114, 1993.
- [94] J. M. Vogels, C. C. Tsai, R. S. Freeland, and S. J. M. F. Kokkelmans. *Phys. Rev. A.*, 56:R1067, 1997.
- [95] Yu. Kagan, E. L. Surkov, and G. V. Shlyapnikov. *Phys. Rev. Lett.*, 79:2604, 1997.
- [96] E. A. Donley, N. R. Claussen, S. L. Cornish, J. L. Roberts, E. A. Cornell, and C. E. Weimann. *Nature*, 412:295, 2001.
- [97] P. O. Fedichev, Y. Kagan, G. V. Shlyapnikov, and J. T. M. Walraven. *Phys. Rev. Lett.*, 77:2913, 1996.
- [98] H. M. J. M. Boesten, J. M. Vogels, J. G. C. Tempelaars, and B. J. Verhaar. *Phys. Rev. A.*, 54:R3726, 1996.
- [99] N. R. Newbury, C. J. Myatt, and C. E. Wiemann. *Phys. Rev. A.*, 51, 1995.
- [100] J. L. Roberts, N. R. Claussen, J. P. Burke, Jr. Chris H. Green, E. A. Cornell, and C. E. Weimann. *Phys. Rev. Lett.*, 81:5109, 1998.
- [101] Ph. Courteille, R. S. Freeland, D. J. Heinzen, F. A. van Abeelan, and B. J. Verhaar. *Phys. Rev. Lett.*, 81:69, 1998.
- [102] S. L. Cornish, N. R. Claussen, J. L. Roberts, , E. A. Cornell, and C. E. Weimann. *Phys. Rev. Lett.*, 85:1795, 2000.
- [103] S. Inouye, M. R. Andrews, H. J. Meisner, D. M. Stamper-Kurn, J. Stenger, H. J. Miesner, and W. Ketterlee. *Nature*, 392:151, 1998.

- [104] V. Vuletić, A. J. Kerman, C. Chin, , and S. Chu. *Phys. Rev. Lett.*, 82:1406, 1999.
- [105] M. Wouters, J. Tempere, and J. T. Devreese. *cond-mat/0305235*, 2003.
- [106] H. T. C. Stoof, J. M. Koelman, and B. J. Verhaar. *Phys.Rev. B.*, 38:4688, 1988.
- [107] H. Feshbach. *Ann. Phys. (N.Y.)*, 19:287, 1962.
- [108] S. K. Adhikari. *cond-mat/0407032*.
- [109] E. Lundh, C. J. Pethick, and H. Smith. *Phys. Rev. A.*, 58:4816, 1998.
- [110] Y. Castin and R. Dum. *Phys. Rev. A.*, 57:3008, 1993.
- [111] P. Rosenbusch, V. Bretin, and J. Dalibard. *Phys. Rev. Lett.*, 89:200403, 2002.
- [112] W. H. Press, S. A. Teuskolsky, W. T. Vatterring, and P. B. Flannery. *Numerical Recipes*. Cambridge University Press, Cambridge, 1992.
- [113] P. Hohenberg and W. Kohn. *Phys. Rev*, page 864, 1964.
- [114] W. Kohn and L. J. Sham. *Phys. Rev*, page 1133, 1965.
- [115] E. Strepparola, R. Nifosi, and M. P. Tosi. *J. Phys.: Condens. Matter*, 10:11645, 1998.
- [116] S. Moroni and G. Senatore. *Phys.Rev. B.*, 44:9864, 1991.
- [117] C. N. Likos, S. Moroni, and G. Senatore. *Phys.Rev. B.*, 55:8867, 1997.
- [118] A. P. Albus, F. Illuninati, and M. Wilkins. *Phys. Rev. A.*, 67:063606, 2003.
- [119] E. Tiesinga, A. J. Moerdijk, B. J. Verhaar, and H. T. C. Stoof. *Phys. Rev. A.*, 46:R1167, 1992.

- [120] E. P. Wigner. *Phys. Rev.*, 46:1002, 1934.
- [121] C. Yannouleas and U. Landman. *Phys. Rev. Lett.*, 82:5325, 1999.
- [122] K. Kärkkäinen, M. Koskinen, S. M. Riemann, and M. Manninen. *Phys.Rev. B.*, 70:195310, 2004.
- [123] I. Romanovsky, C. Yannouleas, and U. Landman. *Phys. Rev. Lett.*, 93:230405, 2004.

